MAJOR PROJECT-II

"Modeling and static analysis of femur bone CT scan data for designing of artificial femur for implant"

Submitted by:

MANJEET KUMAR NAR

M TECH (BME)

2K13/BME/15

Under the supervision of

Prof. B. D. Malhotra

Department of Biotechnology
Delhi Technological University
(Formerly Delhi College of Engineering)
Delhi-110042, INDIA

Abstract

Name of Student: Manjeet Kumar Nar Roll no: 2K13/BME/15
Degree for which submitted: M.Tech. Biomedical Engineering
Thesis Title: Modeling and static analysis of femur bone CT scan data for designing of artificial femur for implant.
Name of Thesis Supervisor: Prof. B.D.Malhotra
Month and year of thesis submission: June, 2015

Hip joint is one of the most important joints in the human body. It is formed by the articulation of femur & acetabulum of the pelvis. It allows us to walk, run, jump and bears our body's weight and the force of the strong muscles of the hip and leg. The finite element analysis (FEA), an advanced computer technique of structural stress analysis developed in engineering mechanics, was introduced to orthopedic biomechanics in 1972 to evaluate stresses in human bones. Since then, this method has been applied with increasing frequency for stress analyses of bones and bone-prosthesis structures, fracture fixation devices and various kinds of tissues other than bone. The objective of this study is the detailed study of hip joint and to develop a 3D robust solid model of femur and analyze with a consistent set of forces of body weight and abductor muscles to validate this developed model under static loading conditions.

Computed Tomography (CT) scan images are used to obtain the geometry of interest. Image processing & computer-aided design (CAD) software tools are employed to obtain the 3D solid model of femur from CT images. Finite Element Analysis (FEA) of robust 3D solid model of femur is done through ANSYS. Results of this study are helpful for the orthopedic surgeon to understand the mechanical behavior of the femur bone and in hip replacement surgeries and implant designing & fixation and can develop a better implant on the basis of these results.

ACKNOWLEDGEMENT

I take this opportunity to express my deepest gratitude and appreciation to all those who have helped me directly or indirectly towards the successful completion of my major project- II.

I express my sincere thanks and deepest gratitude to my guide Prof. B.D.Malhotra Department of Biotechnology, DTU and Co-P.I Mr Sayan Chatterjee, Assistant professor, USBT, GGSIPU, for giving his , sagacious guidance, advice and supervision throughout my synopsis work .I am highly impressed to his intelligence well organised and enthusiastic approach towards goal oriented research . I am privileged to have been his student. I am greatly thankful to him for providing excellent laboratory facilities, perfect scientific environment as well as opportunities to explore scientific world.

I am greatly thankful to all respected faculties of the Department of Biotechnology, DTU for their efficient teaching, generous support and providing me clear concept for research.

I am thankful to my friends and family for throughout provoking discussion and making stay very pleasant.

Manjeet Kumar Nar

CONTENTS

LIST OF FIGURES

LIST OF TABLES

ABBREVATIONS

FEA	Finite Element Analysis
FEM	Finite Element Method
CT	Computed Tomography
CAD	Computer-Aided Design
DOF	Degree of Freedom
DICOM	Digital Imaging and Communications in Medicine
Sip	Simulation Project
NURBS	Non-Uniform Rational B-Splines
HU	Hounsfield Unit
IGES	Initial Graphics Exchange Specification
BW	Body Weight

ABBREVATIONS

Symbol	Definition	Dimension
F	Force	N
K	Stiffness	-
δ	Displacement	M
R	Resultant Force/Vector	N
CG	Centre of Gravity	m/s
W	Weight	Kg
σ	Stress	Pa
ϵ	Strain	-
ρ	Density	kg/m^3
λ	Elastic Modulus	Pa
μ	Linear X-Ray Attenuation Coefficient	-
m	Mass	Kg
g	Gravity	m/s

1. INTRODUCTION

Biomechanics is the study of application of engineering principles and methods to biology in order to preferential understanding of the mechanics of the living systems, particularly their movement and structure. It is closely interwoven with medical physics, physiology, functional anatomy and biomaterials therefore it can be considered as a sub- branch of biomedical engineering (or bio engineering). Biomedical Engineering is an engineering field which combines the concepts of engineering principles and design with medicine and biology for healthcare purposes, including diagnosis, monitoring and therapy.

Biomechanics is not a new field; it came into existence since 1899. Early efforts in this field were made by Aristotle, Galileo and Euler. During the last two decades, development in biomechanics enhanced due to two reasons: first, the development of computers and computational methods in engineering mechanics which realistically describe and successfully analyze complex mechanical behavior of biological tissue; and second, the increasing emphasis on surgical reconstruction of the body parts for disabled and sick.

Biomechanics has participated virtually in every modern advanced technology of medical sciences. It has many fields of application like orthopedic & cardiovascular surgery, traumatology, rehabilitation, dentistry and sports. Thus, it is closely associated with diagnosis, surgery and prosthesis. Long term success of these surgeries and prosthesis requires design and surgical techniques that are based on a sound understanding of human musculoskeletal mechanics.

In this chapter, motivation, aim and scope of this dissertation work are covered.

1.1. MOTIVATION

A joint is an area where two bones are attached for the purpose of permitting body parts to move. Therefore, joints are an important factor in qualitative life. Damage to joints may cause deterioration in the quality of life to a great extent. Hip joint is one of the most important joints in the human body. It is formed by the articulation of femur and acetabulum of the pelvis. It allows us to walk, run, jump and bears our body's weight and the force of the strong muscles of the hip and leg.

Nowadays, fractures and cracks in bones are very common. The most common reason for joint fracture is arthritis and osteoporosis. Between 1990 & 2000, there was nearly a 25% increase in hip fractures worldwide which may increase up to 270% by the year

2050 [1], [2]. It is projected that more than about 50% of all osteoporotic hip fractures will occur in Asia, mostly from most populous countries like China & India, by the year 2050 [1]. According to a recent report, 4.4 lakh Indians suffer from hip fractures annually, while by 2020, it is estimated to record 6 lakhs and the number is expected to increase to a million in 2050. According to the recent Asian audit by the International Osteoporosis Foundation, for every man, three women suffer hip fractures every year in India [2]. Various literatures and surveys reported that the most common site of fracture in hip joint is the femur bone, especially, the femoral neck [3].

Hip fractures are invariably associated with chronic pain, reduced mobility, disability and an increasing degree of dependence. It increases morbidity and mortality rate. So,

the best solution to overcome this problem is the hip replacement or a fixation device. Hip replacement is a surgical approach to replace the hip joint with a prosthetic implant [4]. The goals of hip replacement surgery include increasing mobility, improving the function of the hip joint, and relieving pain. It can be performed as a 'total replacement' or a hemi (half) replacement. The longevity of the THR is determined by the stress distribution on hip joint & prosthesis after THR.

The first hip replacement surgery in India was performed around 1970. In India, over 25,000 joint replacements are performed each year, in which, over 10,000 total hip replacement surgeries are performed each year [5]. The rest of the sufferers in India cannot go through fixation & replacement surgeries due to the high cost of implant & surgery. A success rate of 99% in joint replacements has been shown until now with some limitations [5]. Failure of a hip replacement requiring revision surgery occurs at a rate of approximately 1% per year for the first 15 years [6]. The reasons of failures are: loosening of the component, infection, technical errors at the time of surgery, or recurrent dislocation. Loosening of components is the most common reason for implant failure, causing approximately 75% of failures [7].

In order to better understand the mechanics of joints and bone and to improve the prosthetic component, different types of studies, in vivo[1] and in vitro[2] were performed but due to the limitations of in vivo and in vitro studies, geometry based numerical models have been increasingly considered to better understand the mechanics of the joint (or bone). Potentially, these in silico[3] studies of the joint (or bone) may provide an effective tool for analysis of the joint mechanics & stability, helping researcher & clinician to make confident surgical decisions [8]. In silico methods provide results which were enough automated, had intrinsic accuracy, robustness & generality to be used in clinical applications.

Finite element analysis, first proposed by Professor Clough from the United States in 1960, is a numerical technique for finding approximate solutions to boundary value problems. Applications of this technique in medicine have mainly been in the analysis of structural mechanics and the characteristics of materials. It is a widely accepted tool for 'in silico' studies that is used to study and analyze the mechanical properties of biological structures and Computed Tomography (CT) has been increasingly adopted in FE modeling of a bone [9] as it gives quite an accurate quantitative information on bone geometry which can also be related with the mechanical properties of bone tissues [10], [11]. Research on the Finite Element Analysis (FEA) of the hip joint, implants & fixation devices is not new to orthopedic mechanics. While previous studies have provided a valuable insight into the FEA of the hip joint, implants & fixation devices, they require further enhancement and time to time check which can overcome all the failures and limitations of these replacement surgeries, implants & fixation devices.

1.2. AIM OF THE RESEARCH

The above discussion renders the following conclusions which help in deciding the aim:-

(i) Rate of Hip fractures and replacement surgeries is high in number so it needs a deep consideration and time to time check to cut out the failures and limitations.

(ii) Geometric modeling is an effective way to better understand the mechanics of the anatomical structures.

(iii) Computed Tomography is an effective method to develop a geometry based model.

(iv) Computational analysis results are more accurate and real which can be helpful in orthopedic mechanics applications.

(v) Finite Element Analysis has been widely accepted as a technique for computational analysis that accounts for the complexity of biological structure geometry and its material distribution.

Hence, the aim of this study is to develop a 3D robust solid model of femur and analyze with a consistent set of forces of body weight and abductor muscles to validate this developed model under static loading conditions.

The results of this study shall be helpful for an orthopedic surgeon to understand the mechanical behavior of the femur bone, in hip replacement surgeries and implant designing & fixation. It can also be used as a database for the forthcoming students who are interested to work further in this field of biomechanics.

1.3. SCOPE OF THE RESEARCH

In order to achieve this aim, following steps were followed:-

(i) Acquire lower limb Computed Tomography (CT) scan images.
(ii) Process and Segment CT images to acquire the region of interest, i.e., femur bone by using ScanIP 6.0 software.
(iii) Generate a 3D NURBS surface model of segmented region of interest with the help of ScanIP 6.0 and export in Creo 2.0 for assembly and construction of 3D zones of femur.
(iv) Last but not the least; validate the developed model by analyzing the mechanical behavior under static loading, FE Analysis was done in ANSYS R14.5.

Computational analysis can be performed for longevity estimation of fractured bone or a bone damaged by orthopedic disorders (osteoporosis) and pre-clinical practice during hip-arthroplasty and implant fittings. So, these results are expected to be helpful for a researcher & clinician as pre-clinical information. However, irregular geometry, complex microstructure of biological tissue and loading situations are specific problems of the FEM in biomechanics and are still difficult to model [12]. The aim of this dissertation is to represent a novel method to develop and validate computational models of the femur or hip joint which results in models that certainly have direct clinical applicability to study the mechanics of the joints.

2. THEORETICAL BACKGROUND

The objective of this chapter is to provide a basic relevant theoretical outline of the anatomy and function of the hip joint and femur, biomechanics associated with the lower extremity and finite element method used to solve the problems. It will serve as the reference to the topics described ahead.

2.1. ANATOMY AND FUNCTION OF HIP JOINT

Hip joint (scientifically referred to as the acetabulofemoral joint) is the joint between the femoral head and acetabulum of the pelvis, as shown in Figure 2.1. It's commonly known as a ball & socket joint. It forms the primary connection between the lower limbs and skeleton of the upper body primarily to support the weight of the whole body in both static & dynamic postures.

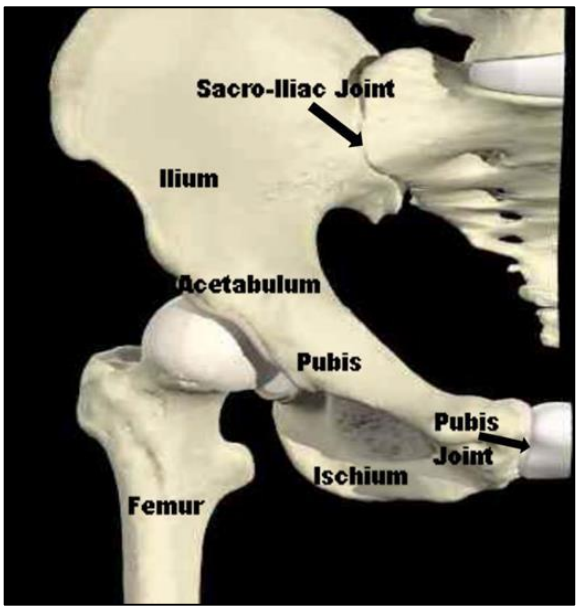

Figure 2.1. Photograph of a plastic hip showing the individual bones and joints [13].

It is also classified as a diarthrodial or synovial joint. Diarthrodial joint contains synovial fluid. Between both the femur and acetabulum synovial cavity is present that contains synovial fluid for lubrication, shock absorbing & joint nourishment, which is surrounded by articular capsule to integrate the two articulating bones. Both the femur and acetabulum are also covered by a hyaline (articular) cartilage whose function is to absorb shock & reduce friction during movement. Several ligaments connect the pelvis to femur to further stabilize the joint and capsule. Muscles and tendons provide actuation forces for the entire range of motion except gliding.

2.1.1. ACETABULUM

The pelvis forms a girdle which connects the spine (or backbone) to the lower limbs providing protection to the digestive and reproductive organs. It is formed by three bones: the ilium, ischium and pubis, which fuse together to form the Os coxae, or innominate bone, as shown in Figure 2.1. At the point of fusing, they form the cotyloid cavity called acetabulum. So, Acetabulum is a concave (cup-like) surface of the pelvis in which femur head is fitted to form hip joint. Each of these bones makes up approximately one-third of the acetabulum.

2.1.2. FEMUR

The femur is the longest and the strongest bone in the human body which consists of a head and a neck proximally, a diaphysis (or shaft), and two condyles (medial and lateral) distally. Its length is about 27% of the person's height. The long bones of the lower extremity, that is, femur may be considered as having two main functions: (i) as a support structure which transfers body weight from hip joint to the knee joint, and (ii) structures on which muscles may act to generate motion. Both of these functions require the bone to be stiff and deform negligibly [14].

Figure 2.2. shows a sketch of a long bone. The diaphysis (shaft) of the femur is a simplistic cylindrical structure, while the proximal femur is irregular in shape, consisting of a spherical head and neck with lateral bony projections termed as the greater and lesser trochanters.

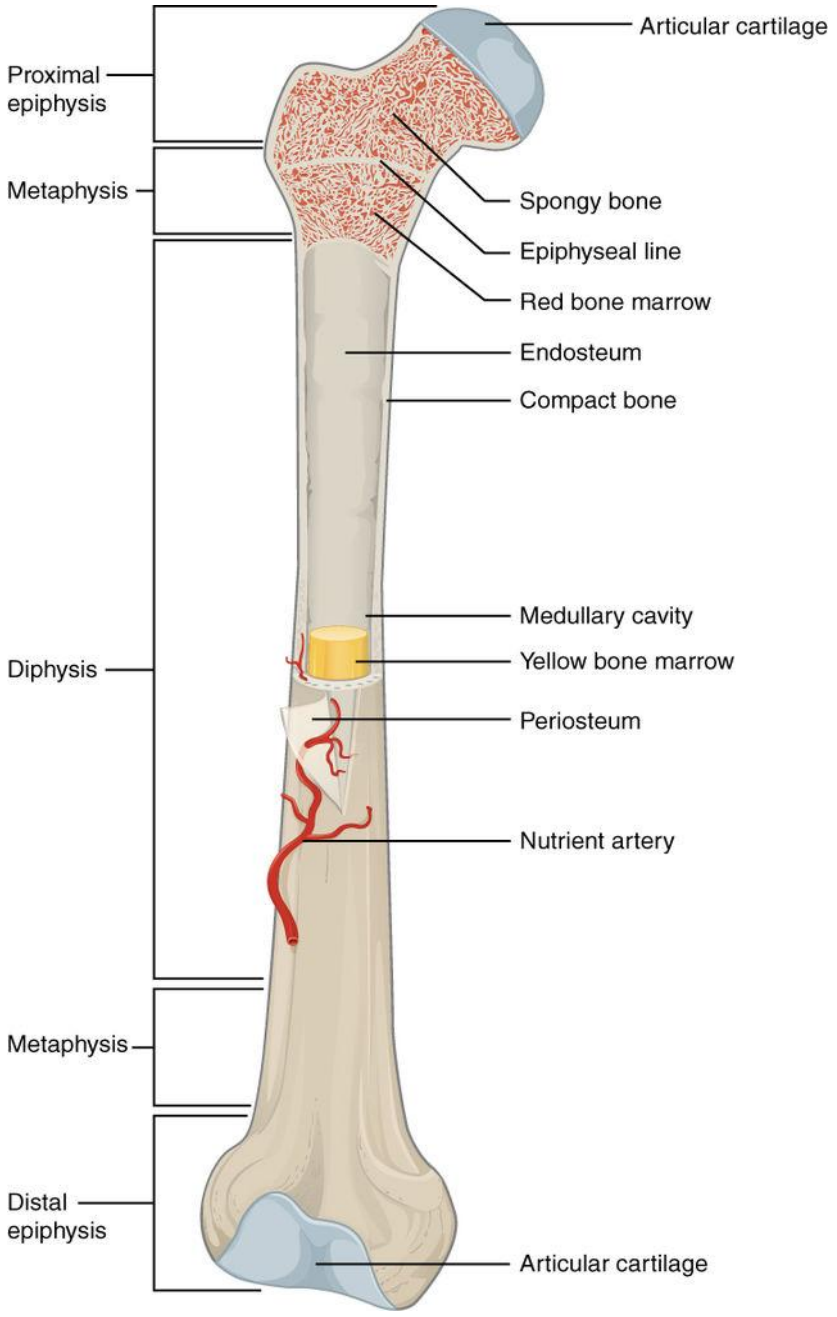

Figure 2.2. Sketch of a long bone, femur [15].

The trochanters serve as the location where major muscles attach. The lateral position of these structures offers a mechanical advantage to assist with abducting the hip [16].

The distal femur is having two round prominence like projections called condyle, medial and lateral condyle. The medial (inner) condyle is larger than the lateral (outer) condyle due to more weight bearing caused by the center of gravity being medial to the knee. Periphery of each epiphysis is covered with a smooth layer of articular cartilage forms the sliding surface of the joint.

When examined at the macroscopic level, long bone consists of two distinct types of bone tissue, cortical (compact) and cancellous (spongy or trabecular). Compact bone tissue is a low porosity and high stiffness dense material forming the extremely hard outer shell of epiphyseal and the diaphyseal regions of the long bones while the cancellous bone tissue comprises of high porosity and directional dependent stiffness thin plates (trabeculae) in a loose mesh structure enclosed by the cortical bone [17]. The periosteum is a dense fibrous membrane that covers the entire bone except joint surfaces which are covered by the articular cartilage. During immaturity, cells of periosteum are responsible for circumferential enlargement and remodeling of the growing long bone, hence it is also known as osteogenic layer.

At the microscopic level, bone/osseous tissue is the major structural and supportive connective tissue of the body that forms the rigid part of the bone organ that frame the skeletal system. It is a mineralized connective tissue formed by cells called osteoblasts that deposit a matrix[4] of collagen fiber and also release calcium, magnesium and phosphate ions. It finally combines within the collagenous matrix into a crystalline material, known as bone mineral, in the form of hydroxyapatite [Ca_{10} ($P0_4$).OH2]. Due to the combination of hard mineral and flexible collagen bone is harder and stronger in nature [18].

2.1.3. LIGAMENTS & LABRUM

Ligament is a fibrous tissue which connects one bone to the other bone. The hip joint has a fibrous joint capsule reinforced by three ligaments. The three ligaments are the iliofemoral, pubofemoral, and ischiofemoral ligaments. The stability of the hip is increased by these three strong ligaments which enclose the hip.

(a) Iliofemoral ligament or the “Y ligament of Bigelo” is attached from the pelvis to the femur and resists excessive extension, as shown in Figure 2.3. (a). It is the strongest ligament in the human body and allows one to maintain a posture for extended periods without extensive muscular fatigue. It supports the hip anteriorly, resists extension, internal rotation and some external rotation [13].

(b) Pubofemoral ligament is attached to the pubic bone and passes inferolaterally to merge with the iliofemoral portion of the fibrous capsule (attaching to intertrochanteric line), as shown in Figure 2.3. (a) [13]. This ligament prevents over abduction of the hip joint.

(c) Ischiofemoral ligament is attached from the ischium to the posterior neck of the femur, as shown in Figure 2.3. (b). It supports the posterior aspect of hip capsule and resists adduction and internal rotation. All the above three ligaments loose during flexion.

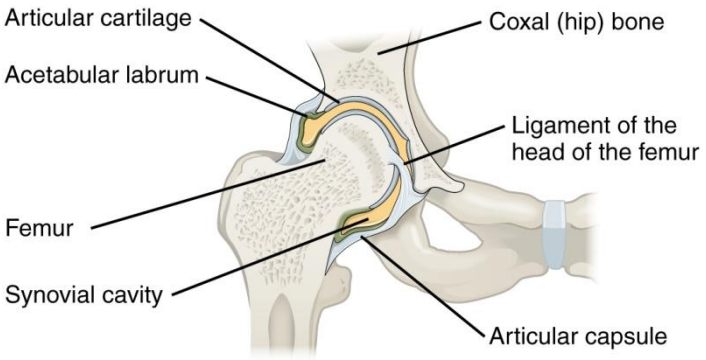

(a) Frontal section through the right hip joint

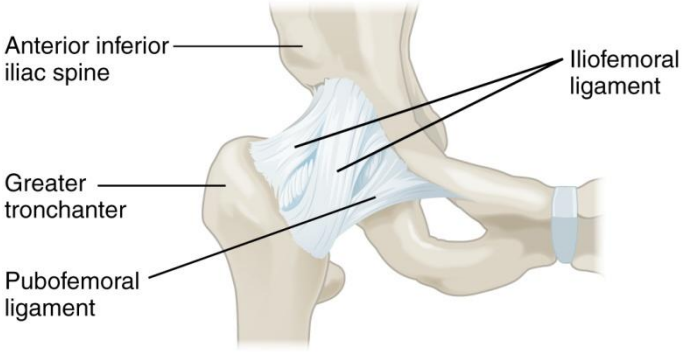

(b) Anterior view of right hip joint, capsule in place

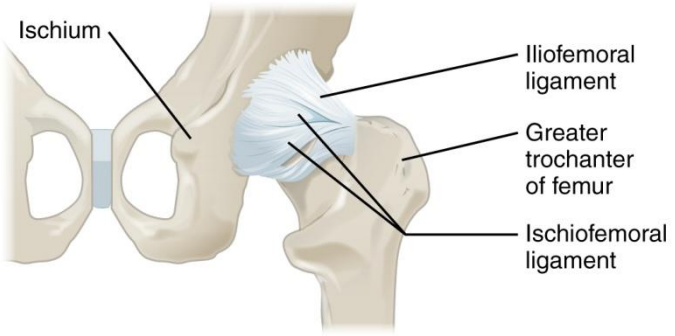

(c) Posterior view of right hip joint, capsule in place

Figure 2.3. Illustration of Hip joint Ligaments [19]

Acetabulum is not a complete circle, open inferiorly so this opening is closed by the transverse ligament, as shown in Figure 2.4. (a). It is a portion of the acetabular labrum. The head of the femur is connected to the acetabulum by the ligamentum teres, as shown in Figure 2.4. (b). It serve as an important channel to supply blood to the head of the femur. However, its contribution decreases with age so it is important in children and is presumably insignificant in elderly patients. Finally, the hip joint labrum (also referred to as cotyloid ligament in older texts) is a ring of cartilage that surrounds the acetabulum, as shown in Figure 2.4. b). Its function is to deepen the acetabulum in order to prevent slipping of femoral head out of the socket and it also helps to guide normal motion.

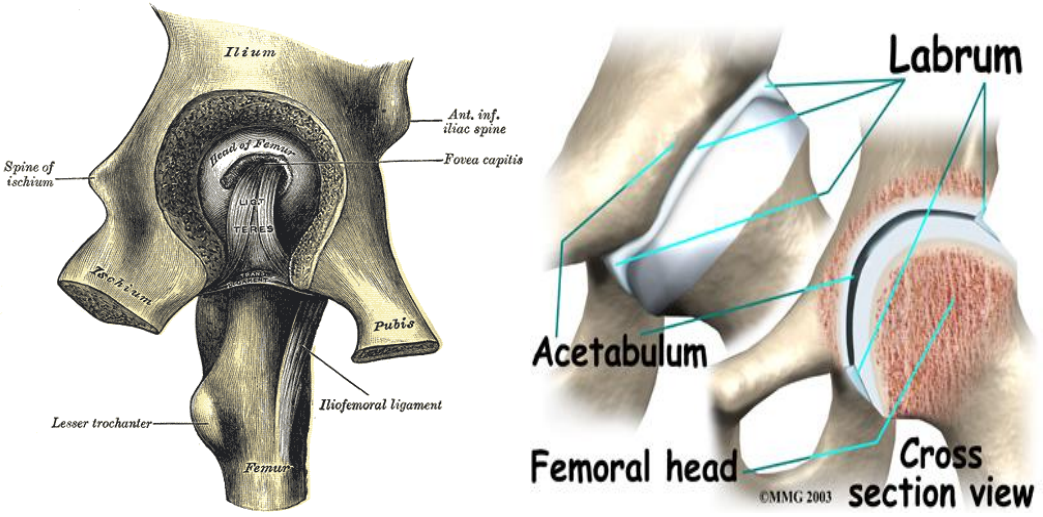

Figure 2.4. Illustration of a) Transverse Ligament, b) Ligamentum teres & Labrum [19].

2.1.4. MUSCLES

Several muscles are attached between the pelvis and femur which is responsible for the easy hip movement and balancing the whole body weight, as shown in Figure 2.5. Many of the hip muscles are responsible for more than one type of movement in the hip, as different areas of the muscle act on tendons in different ways.

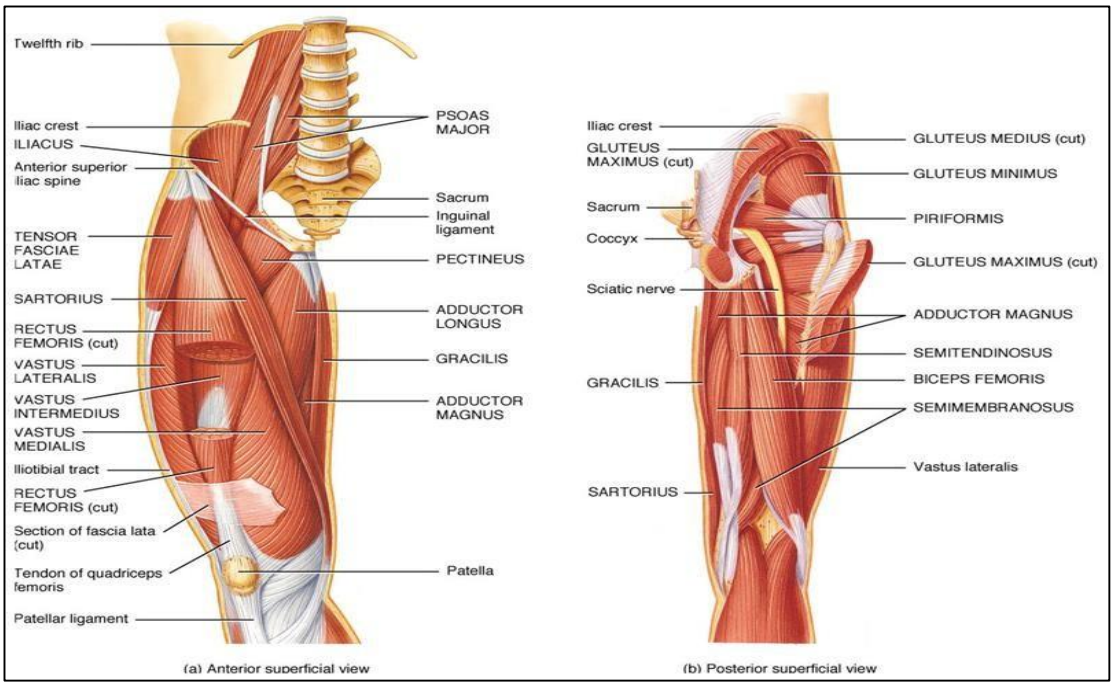

Figure 2.5. Illustration of Hip joint Muscles a) Anterior view, b) Posterior view [20].

Hip joint flexion primarily encompasses due to the psoas, assisted by the iliacus. The pectineus, the adductors longus, brevis, and magnus, as well as the tensor fasciae latae are also involved in flexion. The gluteus maximus and hamstring muscles are responsible for hip extension, but the inferior portion of the adductor magnus also plays a role. Abduction primarily occurs via the gluteus medius as well as the gluteus minimus. The adductor group is responsible for hip adduction. Rotators which are responsible for medial rotation are the gleutus medius and minimus, as well as the

tensor fasciae latae and assisted by the adductors brevis and longus and the superior portion of the adductor magnus, while lateral rotation of hip and thigh is carried out by lateral rotator group. Finally, lateral rotator group includes piriformis, inferior gemelli, externus & internus obturator, quadratus femoris and long & short head of biceps femoris. These muscles are aided by the gluteus maximus and the inferior portion of the adductor magnus. All muscles of the hip with their location and action given in Table 2.1.

LOCATION	MUSCLE	ACTION
Anterior (front) side of the hip	1. Major Ilipsoas 2. Minor Ilipsoas	Flexion
	3. Pectineus	➢ Flexion, Adduction
	4. Iliacus	➢ Flexion
	5. Tensor Fasciae Latae	➢ Flexion, Medial rotation
Posterior (back) side of the hip	1. Gleutus Maximus 2. Hamstring Muscles	Extension
	3. Piriformis 4. Inferior Gemelli 5. Externus & Internus Obturator 6. Quadratus Femoris 7. Biceps Femoris (Short Head) 8. Biceps Femoris(Long Head)	Lateral rotation of hip & thigh
Medial side of the hip	1. Adductor Brevis 2. Adductor Longus	Adduction, Flexion & Medial rotation
	3. Adductor Magnus 4. Gracilis	➢ Adduction, Flexion & Extension
		➢ Adduction
Lateral side of the hip	1. Gleutus Minimus 2. Gleutus Medius	Abduction & Medial rotation

Table 2.1. Muscles of the Hip Joint with their location & action.

2.1.5. HIP GONIOMETRY

Since hip joint is a triaxial joint, it provides a range of motion in all three planes, i.e., the sagittal, frontal and transverse, as shown in Figure 2.6. Flexion, extension and hyperextension all are performed in sagittal plane, with about 140 degrees of flexion, and 15 degrees of hyperextension. Abduction and adduction occur in the frontal plane with about 30 degrees of abduction and 25 degrees of adduction (hyperadduction). Medial and lateral rotation occur in the transverse plane and about 45 degrees of both motions are possible [21].

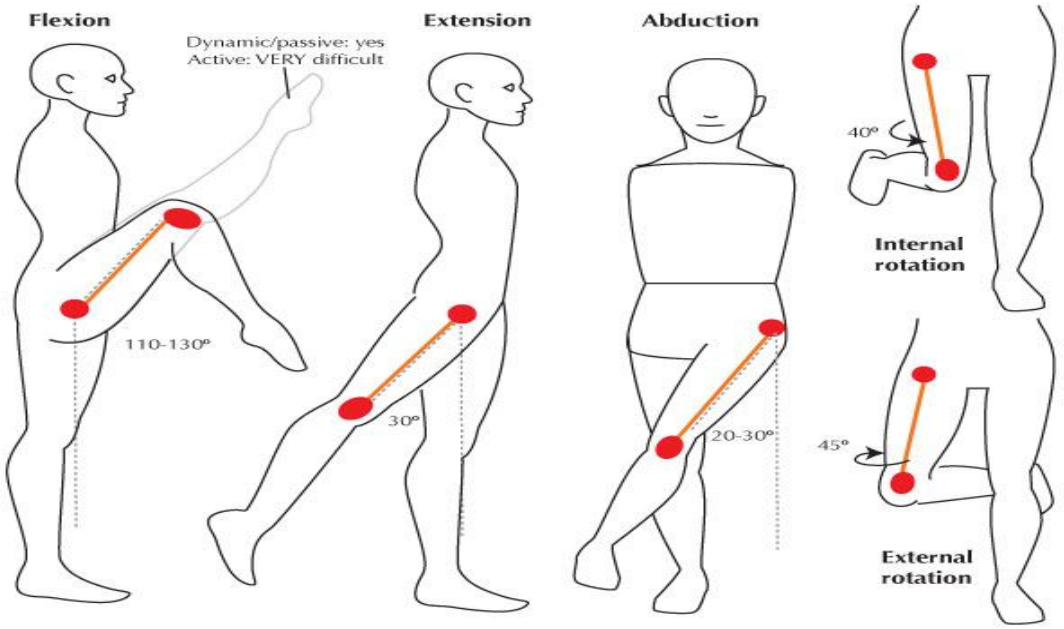

Figure 2.6. Illustration of Different Hip Movements [22].

Because hip joint is congruous, rotation occurs in all directions but there is limit by capsule. As capsule is relatively slack in neutral position, but fibers tighten during rotation[22].

2.1.6. THE NECK-SHAFT ANGLE

The angle formed between the neck and shaft of the femur is called angle of inclination when viewed from front, as shown in Figure 2.7. An oblique angle formed by femoral neck angle with axis drawn through shaft of femur is called angle of inclination with a average of 135 degrees. When the angle of inclination is greater than 135 degrees then this is an abnormality called coxa valga or knock-knees (lengthens the limb). It decreases the effectiveness of the abductors by increasing the load on the femoral head and reducing the load on the femoral neck. While if this angle is less than 135 degrees then this is an abnormality called coxa vara or bowlegs (shortens the limb).It increases the effectiveness of the abductors by reducing the load on the femoral head and increasing the load on the femoral neck [22].

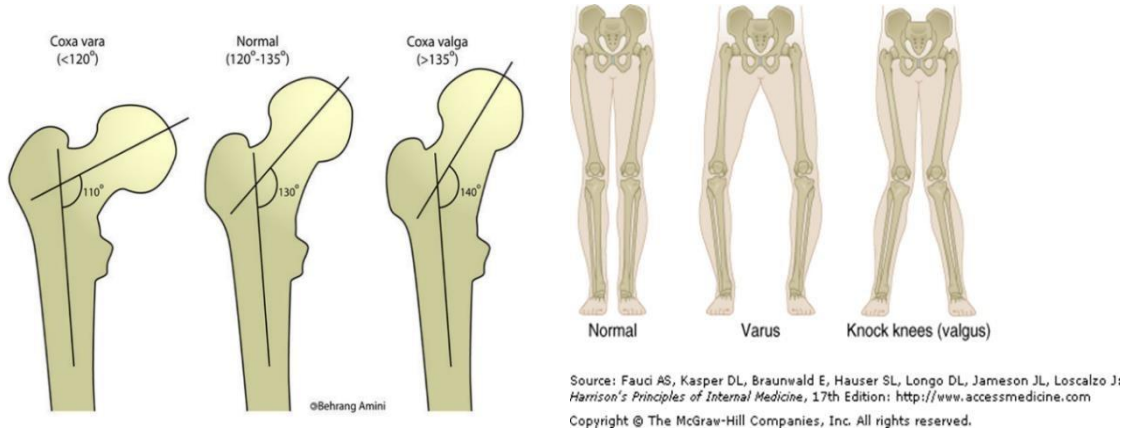

Figure 2.7. Illustration of Neck-Shaft angle of the femur.

2.2. MECHANICAL PROPERTIES OF BONE

Bone is a non-homogenous and anisotropic material that means consist of various cells, organic and inorganic substances with different material properties whose mechanical response depend upon the direction as well as magnitude of the applied load [17]. The major factors that affect the mechanical behavior of bone are:-

(i) The composition of bone,
(ii) The mechanical properties of the tissue constituting the bone,
(iii) The size & geometry of the bone, and
(iv) The direction, magnitude, & the rate of applied loads.

In mechanical terms, bone is a composite consists of an organic matrix and inorganic minerals organized in a hierarchy of structures bridging several length scales [23], [24]. According to Elliott [25], [26] at the nanometer length scale, structure consists of self-assembled collagen fibril (protein) which improves fracture resistance and inorganic hydroxyapatite [Ca_{10} ($P0_4$).OH2] nano-crystals which gives rigidity to the bone and collagen. Bone and its characteristic strength & toughness is imparted by the mechanical properties of the organic and inorganic phases together with their hierarchical arrangement. The compressive strength of bone is relatively high about 170MPa (1800kg/cm2) while tensile strength is poor about 104-121MPa and also very low shear stress strength (5.16MPa), that means it resists pushing forces well, but not pulling or torsional forces. However, bone is essentially brittle in nature; it does have a significant degree of elasticity, mainly contributed by collagen [17].

Bone is a hard complex structural material and has a stress-strain relationship similar to many engineering materials such as metals, polymers, composites. Therefore, a stress analysis of bone can be done in a similar way as to the usual engineering structural analysis [17]. Figure 2.8 shows the stress-strain relationship of a human femur cortical bone.

This σ-ϵ curve is drawn by taking the averages of the elastic modulus, strain hardening modulus, ultimate stress and ultimate strain values calculated for the human femoral cortical bone under tensile and compressive loads with a moderate strain rate in the longitudinal direction by Reilly et al [27]. The curve is showing three distinct regions, linear elastic region, non-linear elasto-plastic region and finally linear plastic region.

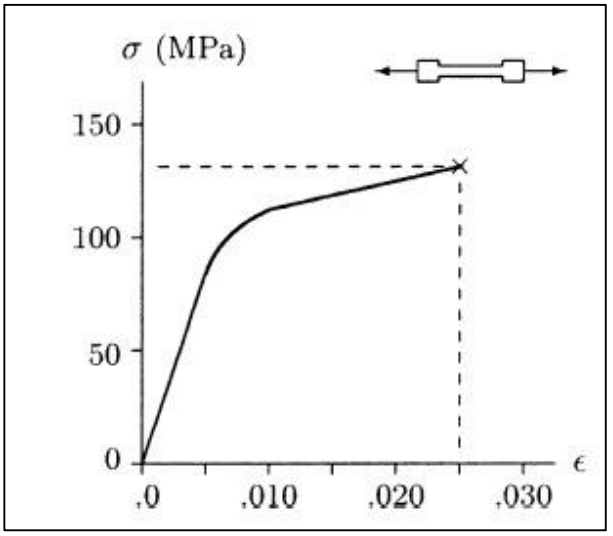

Figure 2.8. Tensile stress-strain diagram for human cortical bone loaded in the longitudinal direction (strain rate $\dot{\epsilon}$=0.05 s^{-1}) [17].

Linear elastic region is a straight line and the slope of which is equal to the elastic modulus of the bone that is about 17GPa. The yield strength of cortical bone, can be determined through non-linear elasto-plastic region of the σ-ϵ curve, is about 110MPa. In the final region, the curve is having another straight line. The slope of this line is equal to the strain hardening modulus of bone tissue which is about 0.9GPa. The bone ruptures when the tensile stress is about 128MPa for which tensile strain is about 0.026. Therefore, the tensile ultimate strength of the human cortical bone is about 128MPa [17], [27].

The chemical composition of cortical and cancellous bone tissues are almost similar but differ in their porosity. For Bones, porosity varies between 10% - 30% for cortical bone while 30% - 90% for cancellous bone [28]. This difference between the two bone tissues can be determined in terms of apparent density, which is defined as the mass of bone tissue present in a unit volume of bone. Figure 2.9 showing compressive stress-strain curve for cancellous bone. It indicates an initial linear elastic region followed by a plateau region approximately with a constant stress until fracture. It exhibits ductile material behavior. Oncontrary abruptly fracture of cancellous bone under tensile force showing a brittle material behavior [17].

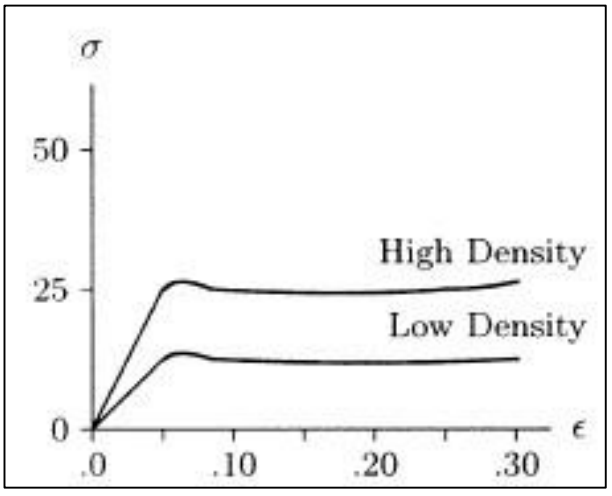

Figure 2.9. Apparent density-dependent stress–strain curves for cancellous bone tissue [17].

2.2.1. ANISOTROPY OF BONE

The stress-strain behavior of bone is also contingent on the orientation of bone with respect to the direction of loading. This anisotropic material behavior is shown in Figure 2.10. indicating that the cortical bone specimens loaded in the transverse direction fail in a more brittle manner than in the longitudinal direction.

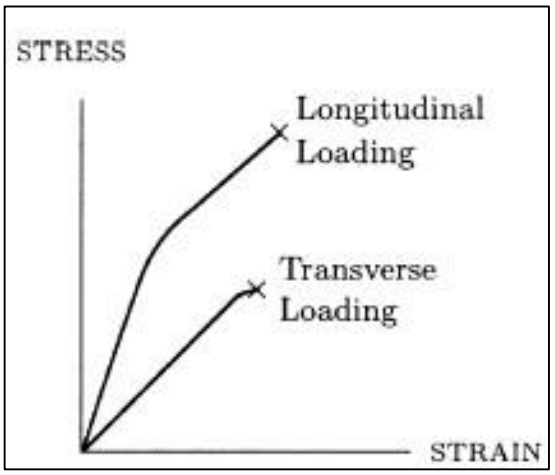

Fig. 2.10 The direction-dependent stress–strain curves for bone tissue [17].

Reilly and Burstein [27] analyzed the mechanical properties of the diaphyseal bone of femur under various modes of loading, as shown in Table 2.2. Table 2.2. [27] indicating that the values of Ultimate strength and elastic modulus of cortical bone is higher in the longitudinal direction rather than in transverse direction that means cortical bone is more stronger and stiffer in the longitudinal direction than in the transverse direction.

Loading Mode	**Properties**	**Femoral cortical bone**
	$E_{Longitudinal}$ (GPa)	17
	$E_{Tranverse}$ (GPa)	11.5
	ρ Density (gm cm^{-3})	3.3
Longitudinal		
	Ultimate Compressive Strength (MPa)	193
	Ultimate Tensile Strength (MPa)	133
	Ultimate Shear Strength (MPa)	68
Transverse		
	Ultimate Tensile Strength (MPa)	51
	Ultimate Compressive Strength (MPa)	133

Table 2.2. Mechanical properties of the femur cortical bone by Reilly et al [27].

(1 GPa = 10^9 Pa, 1 MPa = 10^6 Pa)

Lotz et al. [29] analyzed the anisotropic mechanical properties of the metaphyseal bone. Table 2.3. showing properties of the metaphyseal bone reported by Lotz et al. which can compare with properties of the diaphyseal bone reported by Reilly et al. indicates a major difference.

Properties	Metaphyseal cortical shell
$E_{Longitudinal}$ (MPa)	9650
$E_{Tranverse}$ (MPa)	5470
ρ Density (gm cm^{-3})	1.62

Table 2.3. Mechanical properties of the metaphyseal bone Lotz et al. [29].

2.2.2. FAILURE CRITERIA OF BONE

When bone is under applied load, a small deformation can be seen but when load is removed, bone resumes its original unstressed shape and position showing elastic material behavior. So, deformation directly increases with the increasing load. When the stress generated in any region of bone is larger than the ultimate strength of bone then bone fracture occurs.

It is observed that bone fractures are generally caused due to tensile force but in elderly persons compression is the main cause of bone fracture, while long bone fractures are mostly caused due to torsion and bending [17].

The widely used criteria to check the failure of the structure analysis is von-Mises Yield criterion. In material science, it can be formulated in terms of von-Mises stress or equivalent tensile stress, σ_v, a scalar stress value. When von-Mises stress of a material reaches up to the value of yield strength, σ_y then that material is said to start yielding [30]. Concept of von-Mises stress arises from distortion energy failure theory. According to distortion energy theory, failure occurs when distortion energy in actual case is more than distortion energy in simple tension case at the time of failure. Distortion energy is the energy required for shape deformation of a material [31].
Failure condition can be given by

$$\sigma_v \geq \sigma_y \quad (1)$$

where, von-Mises stress is

$$\sigma_v = [(\sigma_1-\sigma_2)^2/2+(\sigma_2-\sigma_3)^2/2+(\sigma_3-\sigma_1)^2/2]^{1/2} \quad (2)$$

An Arch is formed when weight of the human body is superimposed on the fifth lumbar vertebra & then transferred to the base of the sacrum & across the sacroiliac joints to the ilia, as shown in Figure 2.11. In the standing position of the person the weight of the body is transferred to the acetabula & finally to femora while when a person is sitting the weight is borne on both ischial tuberosities. This means compression on acetabula is caused when a person is standing and compression on ischial tuberosities is caused when a person is sitting [22].

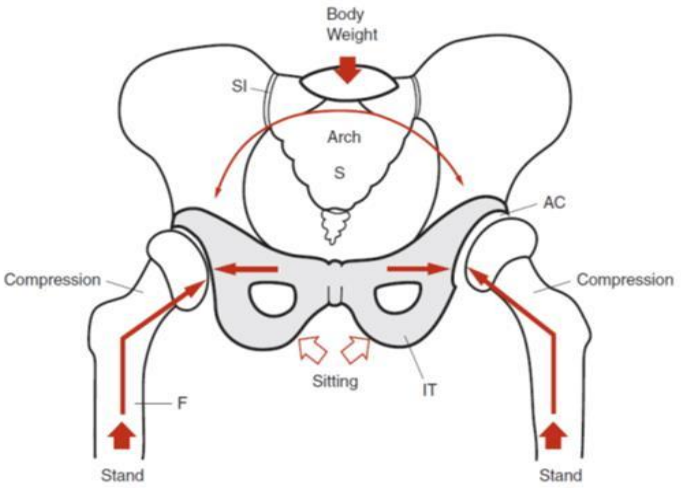

Figure 2.11. Illustration of Weight Bearing of Pelvis Body [Adopted from [22]]. Abbreviations of Figure 2.2.1.Sacrum(S), Sacroiliac joints (SI), Acetabular joints (AC), Femora (F), and Ischial tuberosities (IT).

When body weight is applied on both the legs, the center of gravity lies in the center of the two hips thus exerting equal forces on both hips, as shown in Figure 2.12. Under these loading conditions, the weight of the body minus the weight of both legs is supported equally on the femoral heads, and the resultant vectors are vertical [32], [33].

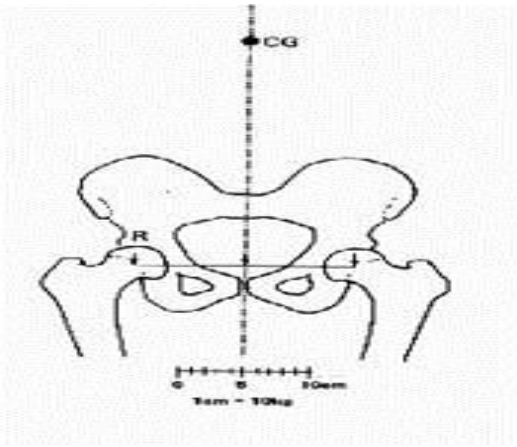

Figure 2.12. Schematic showing the direction and magnitude of the load on the femoral head in symmetrical two-leg stance. [Adopted from [32]].

No muscular forces are required to maintain the balance, albeit minimal muscle forces will be needed to maintain the equilibrium position, when hips are viewed in the sagittal plane and if the center of gravity is directly over the centers of the femoral heads. If the upper body is leaned slightly posteriorly so that the center of gravity comes to lie posterior to the centers of the femoral heads, the anterior hip capsule will become tight, so that stability will be produced by the Y ligament of Bigelow. Hence, the compressive forces acting on each femoral head represent approximately one-third of the body weight in symmetrical standing position on both lower extremities [32].

During the single leg stance phase of gait load applied on the femoral head is approximately 4 times of the body weight due to the combined loading effect of the body weight and the abductor muscles. That means the hip is subjected to wide swings

of compressive loading in normal walking from one-third of body weight in the double support phase of gait to 4 times body weight during the single leg support phase. The factors which is influencing magnitude and the direction of the compressive forces acting on the femoral head are 1) the position of the center of gravity; 2) the abductor lever arm, which is a function of the neck-shaft angle; and 3) the magnitude of body weight, as shown in Figure 2.13.

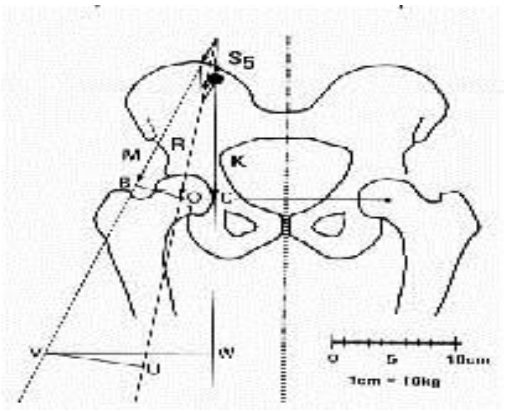

Figure 2.13. Forces on the hip with sideways limping. Note the reduction of vector M and R even though K is unchanged. R is also more vertically oriented. [Adopted from [32]].

For reducing the resultant load on the femoral head another mechanism is to use walking stick in opposite hand. Because some of its force is transferred to the walking stick through the hand thus reducing the effective load of body weight and the turning moment around the femoral head, the abductor demand is also reduced, as shown in Figure 2.14.

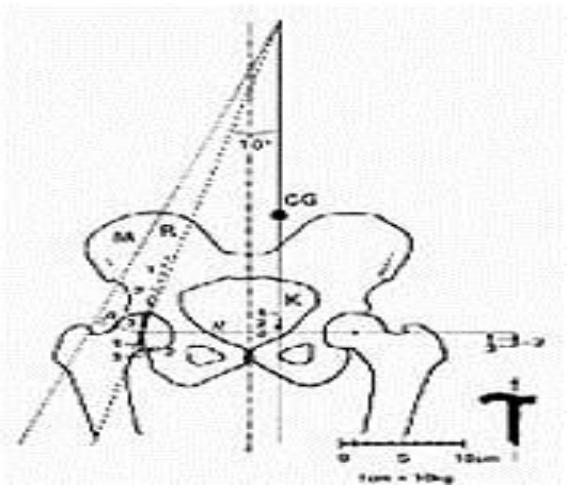

Figure 2.14. Forces on the hip with the use of a cane. [Adopted from [32]].

2.4. FINITE ELEMENT ANALYSIS

Finite Element Analysis (FEA) is an engineering analysis tool, with a wide applications of linear, non-linear, static, dynamic, buckling, thermal, structural and fatigue analysis that is often used in medicines to assist in the design of implants and devices. It is an approximate numerical method that gives mathematical representation of actual

problem. For load carrying structures of unlimited complexity FEA is used to calculate stresses, although there are limitations of a practical nature. All above the method is suited for stress analyses of irregular components as bon-prosthesis structures and is increasing interest in biomechanics research [34], [35], [32].

Minimum number of parameters (motion, coordinates, temp. etc.) required to define position of any entity completely in the space is known as degree of freedom (dof). Any continuous object has infinite degrees of freedom & it's not possible to solve the problem. So, basic theme of FEA is to make calculations at limited (finite) no of points & then interpolate the results for entire domain (surface or volume). Therefore, FEM reduces degree of freedom from infinite to finite with the help of discretization, i.e., meshing (nodes & elements) [36]. Elements are the basic building blocks such as triangle, quadrilateral, tetrahedrons & bricks. Mesh is the collection of elements and nodes are the corners where a number of elements meet.

2.4.1. HISTORY OF FEA

In 1943, R. Courant was the first to give a mathematical foundation for present form of FEA by utilizing the Ritz method of numerical analysis and minimization of variational calculus to obtain approximate solutions to vibration systems. Soon afterwards, M. J. Turner, R. W. Clough, H. C. Martin, and L. J. Topp published a paper entitled "stiffness and deflection of complex structures" in 1956 which established a broader definition of numerical analysis. In the late 60's, mechanical industry recognized FEA as useful tool for solving real life problems. By the early 70's, FEA was limited to expensive mainframe computers generally owned by the aeronautics, automotive, defense, and nuclear industries. In 1972, Brekelmans et al. published a paper titled "new method to analyze the mechanical behavior of skeletal parts", was first introduced in the orthopedic literature after about fifteen years when the finite element method (FEM) initiated a revolution in stress analyses of structure in engineering mechanics. In later 1980's, graphical and computational development took place. Since 1990's FEA has been developed to an incredible precision due to the advent of low cost computers and exceptional increase in computing power [36], [37].

2.4.2. STEPS INVOLVED IN FEA

An analyst can obtain a solution for the stress and strain distribution throughout a continuum when the applied loads, boundary conditions and material properties are known with the help of FE method. The basic steps in any software based finite element analysis consist of the following [36], [38]:

a) Preprocessing Phase

- Creating a 3D CAD Model: Use any of the 3D CAD modeling tools like ProE, Catia, Creo and solid Edge etc. for creating the 3D geometry of the part/assembly of which you want to perform FEA.

- Importing 3D CAD geometry to FEA Package: Start the FEA package and import the CAD geometry into the FEA package like Abaqus, Ansys, and Nastran.

- Defining Material Properties: Define material which is going to be used for the part/assembly in FEA package. By this process, one can define modulus of

elasticity, Poisson's ratio and all other necessary properties required for the FEA.

- Meshing: Meshing is a fundamental step in FEA. In this operation, discretization is used to convert infinite dof to finite elements. So, after this operation the CAD geometry is divided into large numbers of small elements. The small elements are called mesh. The analysis, accuracy and duration depend on the mesh size and orientations. With the increase in mesh size, the finite element analysis speed increases but the accuracy decreases.

- Defining Boundary Condition: Boundary conditions are the loads and constraints that represent the effects of the surrounding environment on the model. Loads can be forces, moments, pressures, temperatures, accelerations and constraints are for resist the deformations induced by the loads. So, by defining where loads applied and where constraints applied to rest the part/assembly

After completion of preprocessing, software internally forms mathematical equations in the form

$$\{F\} = [K]\ \{\delta\} \qquad (2)$$

where, {F} is the vector of applied nodal forces, [K] is a square matrix, known as the stiffness matrix, and {δ} is the vector of (unknown) nodal displacements.

b) Solution Phase

In this step, FEA package solve the problem for the defined material properties, boundary conditions and mesh size. Internally, software carries out matrix formation, inversion, multiplication & solution for unknown, such as displacement & then finds strain & stress for static analysis.

The solution is obtained numerically through a set of linear equations, equal to the amount of degrees of freedom in the model: the number of nodal points times the number of displacement components in each node (two in a 2-D, three in a 3-D model). The processing time and memory space required for a problem in computer progressively depends on the number of degree of freedom. A time-efficient element mesh is crucially important, since computer hardware capacity is the only practical limit to the level of model complexity feasible.

c) Post processing Phase

In this step, FEA package gives results of the solution. The result can be viewed in various formats like graph, value, animation etc. through which you can verify, conclude and think what steps could be taken to improve the design.

2.4.3. ADVANTAGES OF FEA

a) Increases visualization: It is not easy to visualize or predict failure location for real life complex problems but with the help of this tool one can successfully predict failure location for the given set of forces.

b) Decrease design cycle time: Conventional chain design cycle is a very long & time consuming process while current concurrent engineering design cycle is very fast & more efficient due to which design cycle time is decreased.

c) Optimum design: It provides most appropriate environment which results into a favorable design outcome.

2.4.4. ANSYS

ANSYS is a widely used finite element analysis package which can simulate problems in area of structural mechanics, electromagnetics, heat transfer, fluid dynamics, acoustics and coupled problems. It has the capability to analyze static and dynamic, linear and non-linear problems in structural analysis. The simulations carried out in this work are linear static in nature.

Linear static analysis is the most basic type of analysis. The term “linear” signifies that the computed response (displacement, stress or strain) is linearly related to the applied force. And the term “static” signifies that there is no variation of forces with respect to the time or, that the time variation is insignificant and can therefore be safely ignored [39]

3. LITERATURE REVIEW

Since 1972, orthopedic biomechanics has become one of the subjects of interest for research. Significant contributions to understand the human bone mechanics were made by different type of studies like in vivo, in vitro, in silico, and in situ that always help orthopedicians and researchers to do the needful applications for it. Nowadays, numerical modeling, especially computer modeling is widely used by the researchers for this study. Some authors who have done work in a similar fashion adopting different techniques and concluding different results:

In 1973, Frost [40] suggested that the curvature of the long bones, for example, the anterior & posterior curve of the femur has developed in order to prevent bending, thus ensuring that the loads are transmitted axially.

Pauwels [33] was the first to hypothesize that to minimize the bone stresses, muscles were biomechanically important in the reduction of the external bending loads. For this he carried out a theoretical analysis of the loads applied to the entire lower limb during one legged stance. He concluded that when the lower limb was loaded predominantly in bending, the lateral collateral ligament was required to resist a force of approximately two & a half times of the body weight.

Taylor et al. [41] investigated that the femur is loaded primarily in compression and not in bending. The study was carried out in two parts; FEA of intact femur & radiological study. The FE results supported that a compressive stress distribution in the diaphyseal femur can be achieved, producing a consistent stress distribution with the femoral cross-section geometry and both the studies confirmed that during single legged stance negligible deflections of the femoral head experienced for compressive loads. This study also illustrated that however the muscles act to minimize the bending moments but the overall stress distribution is more affected by the direction of the joint reaction force.

Dabrowska et al [42] developed a pelvic bone model in situ[5] through CT data using Mimics and analyze the model on different simulating factors using ABAQUS. Principal stress, Huber von Misses stress and strain energy density were applied as the stimulating factors in remodeling model. The outcome results shown that the non-homogenous pelvic bone model in situ density distribution changes with respect physical properties of bone and also influenced by remodeling simulation procedure.

Radu et al [43] presented an adequate methodology for 3D modeling of hip endoprosthesis. To obtain this they acquired CT data for detailed anatomical information and then virtual modeling was done by using Image processing techniques and 3D computer graphics through Mimics. Finally, they designed a 3D model of hip endoprosthesis using Solidworks with the help of anthropometrical data.

Ghiba et al [44] presented a common solution to overcome the problem of constructing a surface over a set of points cloud data. In order to achieve this, a developed model of the femur extracted through CT data with the help of Mimics software was exported in CAD system, Solidworks, to design a custom made prosthesis and finally check its position in the femur in order to produce an optimal-fit hip stems for individual femurs.

Jun-hai et al [45] simulated stress distribution of femur under bending moment and compressive load using finite element method to understand the failure mechanism. For this study, a two-dimensional FE model of femur was developed according to the dimension of a human femur and analyze for different four excursion lengths, i.e., 0mm, 5mm, 10mm, and 15mm. Thus, it was concluded that stress concentration occurs in femur neck & upper end of shaft, i.e., stress increases significantly with bending moment and tension stress occurs in the outside while the compressive stress occurs in inner side of femur neck.

Trajanovic et al [46] proposed a new method for creating a valid 3D computer surface model of the distal femur, especially for the femoral condyles based on the morphological properties rather than generally used statistical approach for surface model. Thus, a more realistic surface was generated.

Ghiba et al [47] designed a 3D model of coxofemoral joint using CT images divided into eight regions, i.e., pelvis, cartilage, femoral head, proximal femur, distal femur, and shaft. FE analysis of coxofemoral joint model was done in the position of walking monopodal support. It was observed that the stress and strain are very high in proximal femur.

Nareliya et al [48] created a model of real proximal human femur bone with the help of Mimics and ABAQUS. Then behavior of femur bone is analyzed in ANSYS by finite element method (FEM) under physiological load conditions. It was investigated that the mechanical properties vary across the femur bone and with individuals under the physiological conditions. Also showed that higher total displacement observed for higher weights.

Shinge et al [49] analyzed & compared available hip prosthesis with their modified hip prosthesis named as Sancheti Modular Prosthesis (SMP) in which steel head was replaced by Ultra High Molecular Weight Poly-Ethylene (UHMWPE) ball. It was developed for those patients who suffer from the fracture of the neck of femur requiring Partial Hip Replacement. For this, mathematical model was developed for one leg stance and finite element analysis was done by using ANSYS software. They observed that prosthesis using UHMWPE ball is recommended on the basis of equivalent stresses, but on the aspect of displacement UHMWPE ball is found more displacement than stainless steel 316L ball. Hence, UHMWPE is not recommended due to more displacement.

Vulovic et al [50] developed a 3D FE model based on CT scan with different internal zones correspond to the regions with different internal structure by using CATIA software. Then for one-legged stance case static linear analysis of femur surface model was done by PAK software. It was concluded that critical places in a femur as per the analysis result is the femur neck.

Lahari et al [51] generated a 3D model of the osterioporetic, osteriopenic and normal femur bones from the patient specific CT data and various BMD measurements of the developed proximal femur was done by using Mimics. After that finite element analysis was carried out by using ANSYS and then these results compared with the DXA values.

Francis & Kumar [52] created a 3D finite element model of the right proximal femur for three different age group male patients with the help of CT scan data by using Mimics,

for FEA loaded by individual body weight which was shared equally by the lower limbs, at different inclination angles. By using ABAQUS they determined the total deformation, equivalent von-Mises stress, maximum principal stress, fatigue tool and percentage variation and results showed that increase in curvature with age results in the increase of inclination angle which in turn decreases the safety factor.

Datar et al [53] proposed a procedure for analyzing the fatigue life of hip implant for a physical activity of brisk walking with a speed of 2.1 m/s. They developed a three-dimensional FEA model of the implant, consist of femur head and stem, by using Solidworks as per the implant norms set by ISO 7206. Through finite element analysis it was found that induced stresses developed at four different critical locations during brisk walking at a speed of 2.1 m/s. Out of four locations, the location 'Neck Out' is the only point where the stress induced is greater than the endurance strength. So, the fatigue life of implant is defined by this most heavily stressed location on the implant surface. However, the remaining three locations exhibit infinite life in fatigue but due to finite life of the most critically stressed location, overall life of the implant is also become finite. Thus, concluding that the femoral neck is the point of failure in most of the implant cases especially during brisk walking and life of hip implant becomes infinite if the test subject walks at a speed of 1.5 m/s.

Spinelli et al [54] assessed the mechanical behavior of an uncemented hip stem using finite element analysis. They modeled with the three distinct conditions: a) exposed neck with fully embedded fins, b) partially exposed anti-rotational fins and c) fully exposed fins, representing real femoral hip conditions. It was observed that displacement increases directly with the increase of both the length of exposed fins and the magnitude of applied forces, however small displacements noticed in all the three conditions. For static conditions numerical analysis of the used uncemented femoral stem exhibited that small stresses and strains was generated under working load conditions showing that a proper factor of safety is obtained. Thus, it concludes that the risk of hip bone fracture increases due to stem exposure.

Shireesha et al [55] generated a FE model of femur using CT scan data by CATIA software and under static loading conditions analysis was done for the stresses formed in different implant materials, structural steel and Ti-6Al-4V, by using ANSYS software. On comparing these two implant materials analysis result, it was found that Ti-6Al-4V gave less deformation on static loading conditions as it is a low density material. It has excellent biocompatible and mechanical properties which is supposed to be ideal for the use of an implant.

Ghosh et al [56] developed a realistic 3D FE model of the hemi pelvis using CT images and analyze stress and strain distribution generated in particularly the acetabulum during a normal walking. FE model included cortical and cancellous bone and cartilage layer over femoral head. This study is useful for further research on acetabulum prosthesis. High stresses around 40-57MPa were observed in the acetabulum with a spherical head and considerably reduced to 5-10MPa when the cartilage layer was generated.

Cardiff et al [8] alternatively developed a FE model of hip joint based on the sandwich model approach which included cortical & cancellous bone and cartilage layer with the help of 3D Slicer software and then established a procedure for numerical analysis of

hip joint using finite volume method by performing three phases of gait analysis using OpenFOAM, an open source software. It was found that in the mid-stance phase model, the pelvis is relatively highly stressed in the acetabular roof and in the femur more stress is experienced in the area where significant bending occurs.

4. MATERIALS AND METHODS

A common approach to bone modeling for FE analysis was adopted in order to demonstrate the work, i.e., 3D solid model generation and FE analysis of femur. A flow chart indicating step by step work and software used to carry out each step is shown in Figure 4.1. [57].

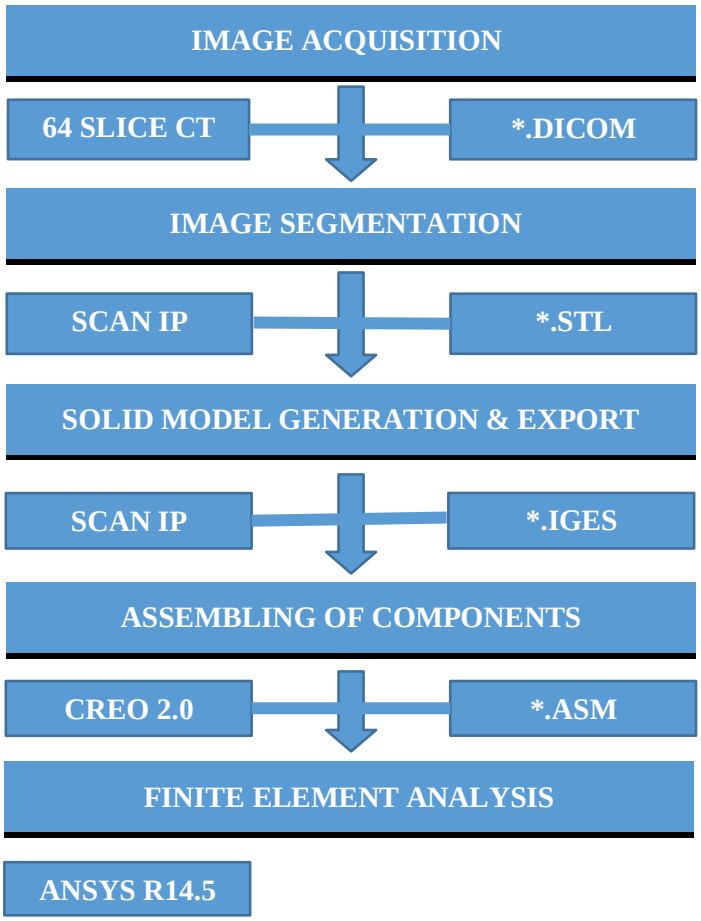

Figure 4.1. Flow chart showing whole research work in steps. The boxes in the left column contain the software tools and the right column boxes indicate the data file extension.

Steps comprising the complete analysis are:

(i) The CT image data that preserves the geometrical information of femur was acquired.
(ii) A 3D surface model was developed using Trialed 8license copy of Simpleware Scan IP 6.0, a robust Image Visualization & Processing software
(iii) Creo 2.0, a CAD package, was used for assembling of femur and
(iv) For the final step to investigate the mechanical behavior of the developed model, FE analysis was done in ANSYS R14.5.

4.1. IMAGE DATA ACQUISITION

In earlier studies, either a frozen (dry) bone, synthetic bone ,a wet bone or a bone with apparent density was used for the analysis but in computational biomechanics, especially for orthopedic applications, CT has been increasingly adopted for bone remodeling since hard tissue has a high contrast relative to soft tissue (cartilage, muscles, ligaments, etc.) [58], [43]. It is well known that CT images can give fairly precise quantitative information on bone geometry which can also be related with the mechanical properties of bone tissues.

CT scan images are a pixel map of the linear X-ray attenuation coefficient of tissues [48]. Each pixel value is scaled so that the linear X-ray attenuation coefficient of air equals to-1000 & that of water equals to 0. This scale is called H.U. scale or CT numbers, after Godfrey, one of the pioneers in CT, shown in Figure 4.2. It is a quantitative scale for describing radio-density, calculated as follows:-

$$HU=1000X(\mu_x-\mu_{water})/\mu_{water} \quad (3)$$

Where, μ_x = Average linear attenuation coefficient in a voxel,
μ_{water}=Linear X-Ray attenuation coefficient of water

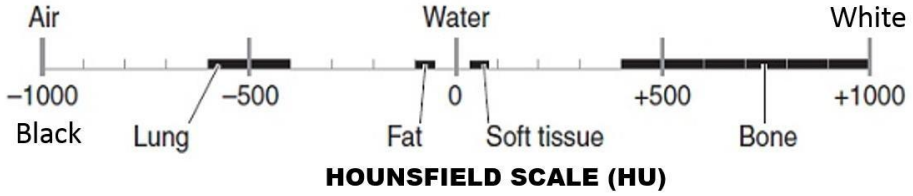

HOUNSFIELD SCALE (HU)

Substance	HU
Air	−1000
Lung	−700
Soft Tissue	−300 to -100
Fat	−84
Water	0
CSF	15
Blood	+30 to +45
Muscle	+40
Bone	+700(cancellous bone)to +3000 (dense bone)

Figure 4.2. Hounsfield scale.

Lower limb CT data of a 56 years old healthy female subject whose body weight is 75 kg was used for this study, provided by 64 SLICE CT–SCAN, Rao Diagnostic Centre, Chatrasangh Chaurha, Gorakhpur, U.P. India. The data acquired have an arterial phase and obtained in a helical mode with a slice thickness of 1 mm from a 64 slice CT scan, GE medical system by aligning the lower extremity of the subject to the CT scanner rotating in clockwise direction, apparatus power condition were at 120KV/350mA.The images obtained in DICOM (Digital Imaging and Communications in Medicines) format consists of 2-D gray scaled images of a human female. It is a standard for handling, storing, printing, and transmitting information in medical imaging. It contains binary data elements. Number of slices obtained are 1286.

4.2. EXTRACTION OF GEOMETRY: IMAGE SEGMENTATION

The second phase of modeling is to extract the geometry of the region of interest, i.e. femur bone from CT data of a female subject. In orthopedic biomechanics, a number of approaches have been used to extract the geometry of interest from CT images such as MIMICS (Materialise Interactive Medical Image Control System), 3D Slicer, ScanIP and Amira. In this study, Simpleware ScanIP was used because it is user friendly, has fast processing and meets our system requirements. ScanIP 6.0 software provides image processing tool to assist the user in visualizing, measuring & segmenting regions of interest from any volumetric 3D data. File format of ScanIP is sip (Simulation Project) which is primarily associated with 'Powersim Studio' by Powersim Software AS.

Powersim studio is an integrated environment for building & running simulation models.

4.2.1. IMAGE VISUALIZATION AND PROCESSING

As the DICOM images are large in size, it is difficult to handle this data without processing. So, the first step in order to get region of interest is image processing. DICOM images of the lower limb were imported to ScanIP 6.0, area of interest was cropped and resampled which reduces number of slices from 1286 to 506 and memory requirement from 257.50 MB to 49.59 MB by making process fast & easier.

Resampling the data to a low resolution at which small features are retained while the overall size of the image is reduced will usually make the segmentation step easier due to lower memory requirements, reduced amount of pixels to process in the case of manual segmentation, and can also reduce the number of elements in the final FE mesh. It can also be useful to artificially increase the resolution by super sampling the data but it will not modify object sizes. While cropping is the simple operation of cutting off parts of the volume in order to only keep data of interest. For memory usage purposes, it is recommended to crop the image in order to only keep the necessary objects within the limits of desired volume [59].

Contrast enhancement can be carried out to improve the model by differentiating bone from other tissues and makes segmentation part easier [42]. It was done by adjusting window width: 850.47 & level: 362.11 in histogram (Greyscale range -2000 to 2000), as shown in Figure 4.3.

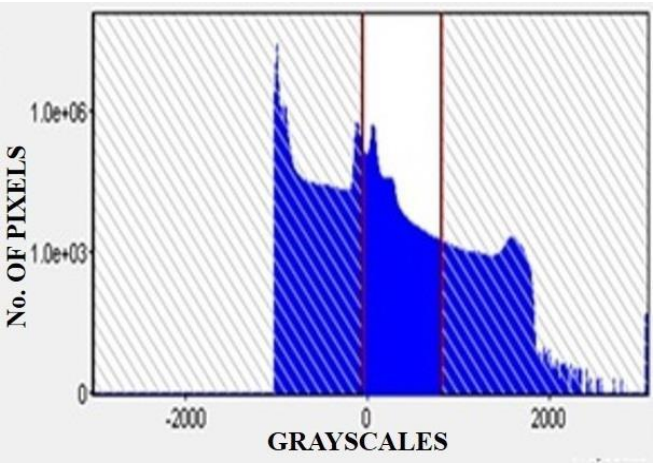

Figure 4.3. Histogram of the acquired data showing gray scale range.

An image histogram is a type of histogram that graphically represents tonal distribution in a digital image [58]. It plots the number of pixels in an image (vertical axis) for each grayscale value or tonal value or brightness value (horizontal axis). Pixels are the basic element of an image and Grayscale values are the values assigned to each pixel in a single sample. It can be visualised as if each pixel is placed in a bin corresponding to the colour intensity of that pixel [59].

4.2.2. IMAGE SEGMENTATION

The next and important step to move towards modeling phase is image segmentation, which can be defined as the process of partitioning a digital image into multiple pixels (sets of pixels, also known as superpixels [60], [61]. It plays an important role in many medical imaging applications to ease the description of anatomical structures and other regions of interest.

In ScanIP 6.0 software, a segmentation tool can be fully manual (Paint), or assisted (Threshold, Paint with threshold, Flood Fill, Region growing). In any case, none of the tools are fully automated, and they will require some expertise and practice in order to give satisfactory results. As multiple segmentation algorithm available for segmentation of images but in this study region growing method for partial automatic segmentation process and for further manual segmentation paint with threshold technique was used. Region growing tool is a simple region-based segmentation. It is used to split the image into different and separate objects [57]. It does not provide complete segmentation at one time but gives a clear view of parts near the complex regions of proximal and distal ends of femur by defining their boundaries. Due to this technique, the next step of manual segmentation becomes easier. Macroscopically, femur bone consist of cortical and cancellous bone. For FE analysis to differentiate between cortical and cancellous bone [9], [11], three different mask color were used, i.e., red mask for cortical bone, turquoise mask for cancellous bone at distal end & green mask at proximal end in femur, as shown in Figure 4.4. It helps in defining different zones in model as a natural bone has.

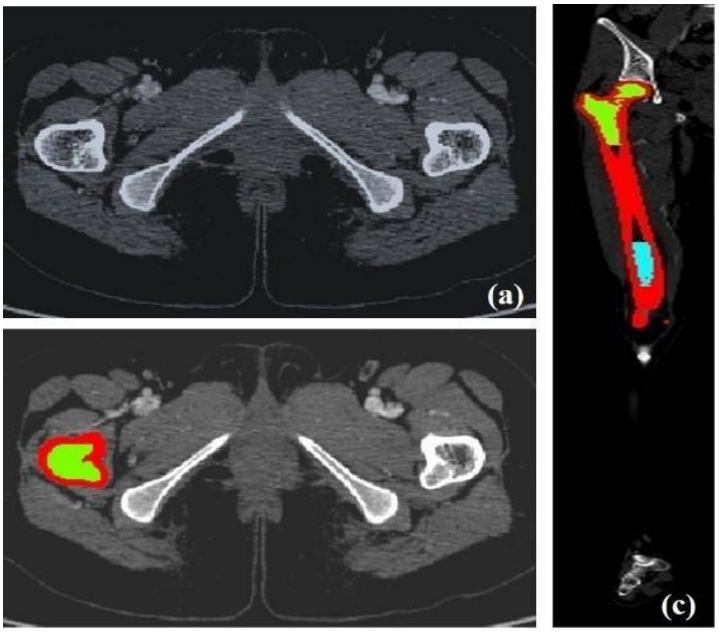

Figure 4.4. a) 2D Tomographical slice b) Segmentation process used to extract region of interest c) Sagittal view of segmented femur by using different mask.

The region growing is applied with number of iterations to be 3, multiplier value of 2.0 and initial neighborhood radius (pixels) of 2 for cancellous bone while number of iterations decreased to 1 for cortical bone. Then manual segmentation is done by adjusting lower and upper threshold value in between 23 to 255 for red mask, 11 to 169 for turquoise mask and 19 to 100 for green mask. Figure 4.5 shows results after application of each segmentation technique.

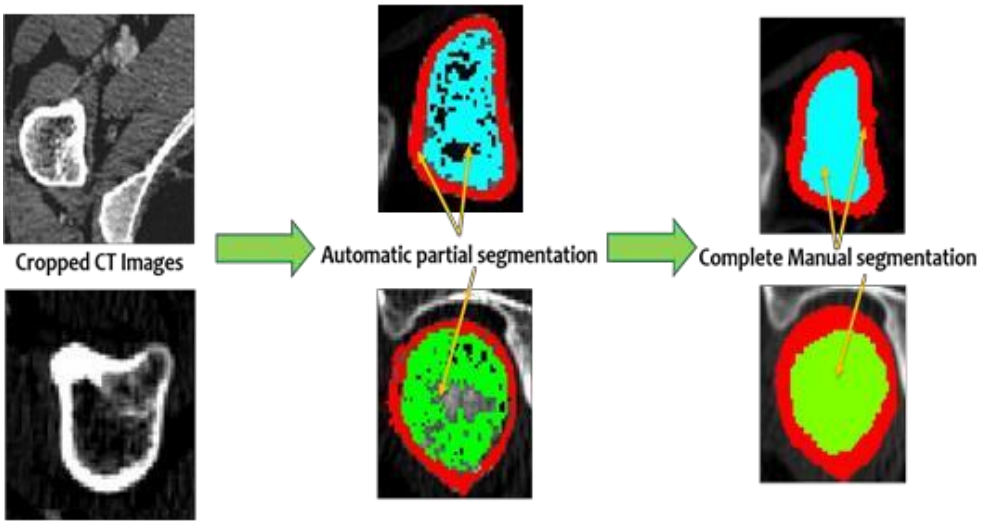

Figure 4.5 Image segmentation tools results on CT data.

4.2.3. IMAGE SMOOTHING

After completing the segmentation part, next phase is smoothing of the obtained segmented region mask as it has rough surfaces and noise, as shown in Figure 4.6. So in order to achieve smooth surfaces and noise free segmented region, smoothing of each mask was carried out using Recursive Gaussian Filter.

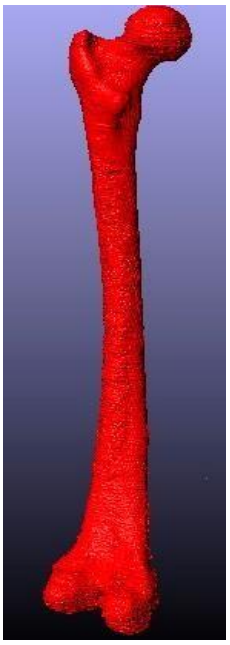

Figure 4.6. 3D view of rough surface of segmented region mask of cortical bone of femur.

Smoothing filters are filters that will get rid of noise and also smooth or attenuate contours by preserving the partial volume effect as greyscale values alone will not be sufficient to smooth the data. Examples of filters that fall in this category are the Recursive Gaussian, Mean filter and Median filter [57]. After applying all these filters on the segmented region mask, a conclusion came out that Recursive Gaussian filter is a powerful way to smoothen the data in comparison to other filters. Recursive Gaussian filter reduces image noise and detail levels. Visually, it has the effect of blurring while mathematically, it has the effect of low pass filtering the image [57].

After applying smoothing operation, data loss was observed at the proximal and distal ends of the femur may be due to the thin cortical layer over there, as shown in Fig.4.7.

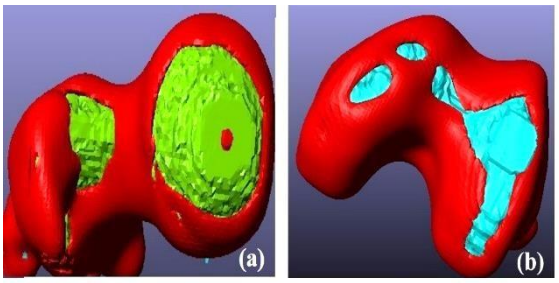

Figure 4.7. Smoothing operation results showing data loss in cortical regions at a) proximal portion of femur b) distal portion of femur.

Due to the implication of data loss, morphological dilate filter of 1 (cubic values) was applied before performing smoothing operation. Morphological dilate filter adds a layer of pixels to both the inner and outer boundaries of regions [57]. Here, morphological dilate filter exactly used to grow the mask of cortical layer so as to remove the effect of data loss and obtain smooth mask of both cortical and cancellous region. Hence, Gaussian sigma of 2.5 (cubic values) was applied on cortical region mask and of 2.0 on the mask of cancellous region, as shown in Figure 4.8.

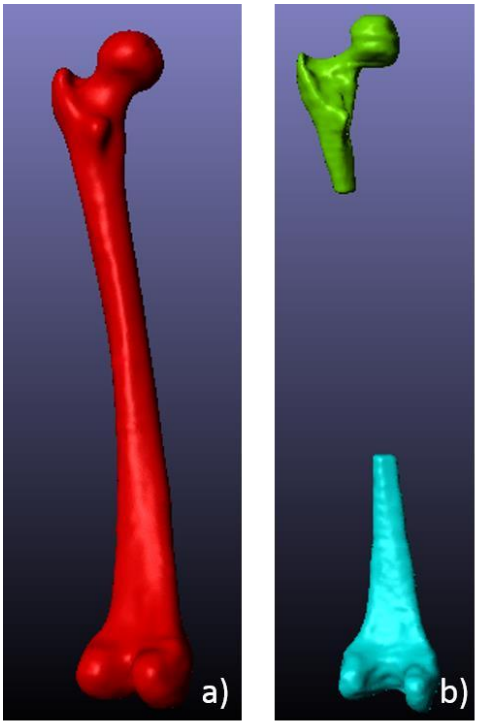

Figure 4.8. 3D view of smooth segmented femur a) cortical region mask and b) cancellous region mask by applying Recursive Gaussian Filter after using morphological dilate.

4.3. GENERATION OF SOLID MODEL

Third and fourth phase of modeling is the generation of solid model which is based on the polygonal modeling.

4.3.1. GENERATION OF SURFACE MODEL

Third phase of modeling is the generation of surface model. For this, the generated region mask was used to develop 3D surface model for the bone by using ScanIP 6.0. This was done by selecting a new NURBS (Non-Uniform Rational B-Splines) model and adding segmented region mask into the model. Then, set up the model according to desire and generate a full model. Thus, NURBS surfaces were created from the generated region mask with its associated IGES format, as shown in Figure 4.9, which represent the outer manifold (cortical) of femur and the border of inner medullary cavity.

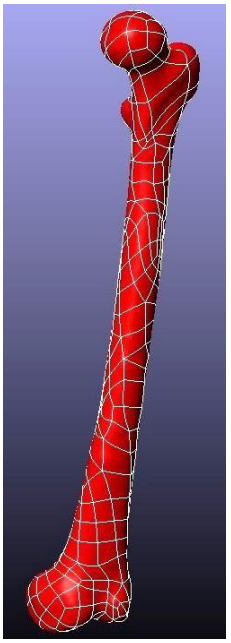

Figure 4.9. NURBS surface model of femur from segmented region mask.

The Initial Graphics Exchange Specification (IGES) (pronounced eye-jess) is a file format which defines a vendor neutral data format that allows the digital exchange of information among Computer-aided design (CAD) systems. The reason behind opting NURBS is that the objects are easy to manipulate interactively, and because the algorithms that create them are both efficient and numerically stable.

After this, export the generated NURBS surface model of femur in IGES format.

4.3.2. ASSEMBLY AND CONSTRUCTION OF 3D ZONES

Fourth phase of modeling is the assembly of femur surface model and construction of 3D zones, based on the polygonal modeling. Assembling of different parts of femur model was done by using Creo Parametric 2.0 software by importing generated NURBS solid model of femur in IGES file format. Creo Parametric is a 3D computer aided design software for parametric featured modeling based on solid modeling. It is also known as Pro/Engineer. Then, the other surfaces of the model were created, using advanced 3D CAD features, which divide the inside of femur model into zones corresponding to regions with different inner structure [62], i.e., proximal and distal region of femur which corresponds to cancellous bone, as shown in Figure 4.10. (b).

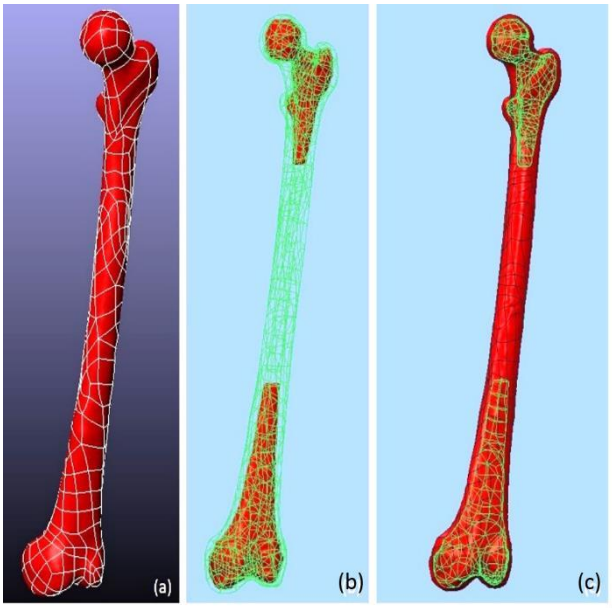

Figure 4.10. Polygonal models (a) NURBS model showing outer cortical region, (b) Model showing outer(cortical) and inner(cancellous) at proximal & distal ends of femur, (c) Model showing solid outer(cortical) and inner(cancellous) at proximal & distal ends of femur.

The construction of three-dimensional zones performed by the use of advanced modeling features in CREO 2.0. Then Solid feature, filling the whole outer manifold has then been created and divided into segments using the NURBS surfaces, as shown in Figure 4.10. (c) with ASM file format associativity.

This model was then exported to ANSYS for the analysis part in ASM file format.

4.4. FE ANALYSIS OF FEMUR

Final stage after modeling was to analyze the developed 3D solid model of femur. Static structural analysis was performed for single legged stance in ANSYS Workbench R14.5. ANSYS, a CAD package, is an engineering simulation software which helps in determining & improving the weak points, computing life & foreseeing probable problems are possible by 3D simulations in virtual environment. In simple language, it is an FE program for linear and non-linear analysis.

4.4.1. FE MODEL OF FEMUR

A 3-D F.E. model was build for static stress analysis by using the ANSYS Software. The constructed femur model was imported from Creo 2.0 to ANSYS software as an ASM file to generate a volumetric mesh. For volumetric meshing of the femur model, tetrahedron automatic mesh generation was used. Meshing is a discrete representation of the geometry in the problem. It assigns smaller regions over where boundary conditions are applied to solve the problem. Tetra meshing is a 3D meshing where tetrahedron, element shape, is a polyhedron composed of four triangular faces, three of which meet at each corner or vertex. It has six edges and four vertices. Three-dimensional finite element Tetra mesh model of femur contains 93,543 elements and 114,137 nodes for the element type solid187, as shown in Figure 4.11.

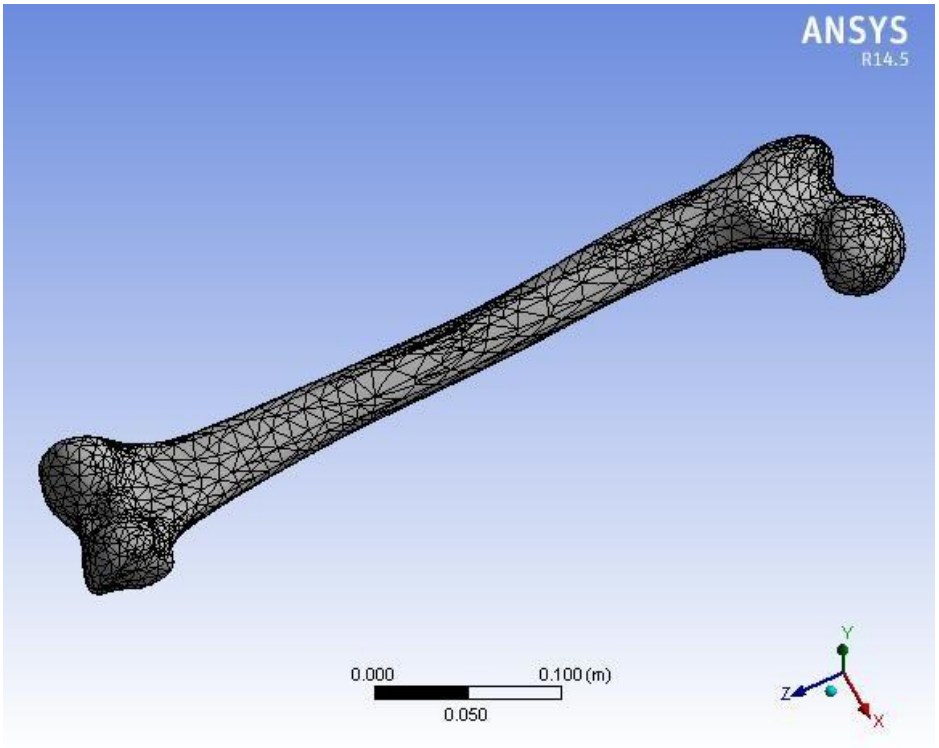

Figure 4.11. FE tetra mesh 3d model of femur contains 93,543 elements and 114,137 nodes for the element type solid187.

Solid element type is a high order 3D, 10 node element. Solid187 has a quadratic displacement behavior & is well suited to modeling irregular meshes such as those produced from various CAD/CAM systems.

4.4.2. MATERIAL ASSIGNMENT

Human bone is highly heterogeneous, anisotropic & non-linear in nature, which means that its properties depend on the direction and location but it is difficult to assign material properties along each direction of bone model. So, in this study bone material behavior was assumed as a homogeneous isotropic linear elastic material, distinguishing between cortical and cancellous bone. The consideration of heterogeneous to homogeneous material helps make FE Analysis, especially meshing part, easier. In this study, material can be assigned in two different ways, either in Creo or in F.E. module.

Here material properties are directly assigned in ANSYS. The average mechanical properties of each type of bone tissue are shown in Table 4.1 which were extracted from CES selector (Cambridge Engineering Selector, an engineering materials selection tool).

Structural Properties of Bone	Value
Young Modulus	1.7e10 Pa
Poisson's Ratio	0.31
Density	1.8e3 kg/m^3
Thermal Expansion	1e-5 /°C
Tensile Yield Strength (elastic limit)	1.2e8 Pa
Compressive Yield Strength	1.14 e8 Pa
Bulk Modulus	* 1.8e10 Pa
Values marked * are estimates	

Table 4.1. Table of the material properties of bone used for the simulations (from CES selector).

According to van Rietbergen et al [63], Bitsakos et al [64], and Verhulp et al [65], material properties used in subject specific models of the femur are derived based on CT (computed tomography) data, where the greyscale values can be converted to an isotropic value for the mechanical properties. So, by using the empirical formula, bone material properties can also be determined through gray values [66], [67],

Density (kg/m^3)

$$\rho = -13.4 + 1017 \times [\text{Gray value}] \quad (4)$$

& Elastic Modulus (Pa)

$$\lambda = -388.8 + 5925 \times \rho \quad (5)$$

The lower boundary of the bone properties was selected for these simulations as the subject age was more than 50 years.

4.4.3. LOADING AND BOUNDARY CONDITIONS

One of the difficulty in geometry modeling of the femur is the anatomical variation between individuals. A further difficulty is the difference in activity patterns and also that activity patterns may change after hip replacement [68]. However, in this study for the purpose of structural stress analysis, full complexity was not considered. Extensive work on the forces transmitted to the hip during gait has been carried out by Paul [69] and Bergmann [70].

Earlier mentioned Figure 2.5. shows the muscles attached to the proximal femur from which its complexity can be appreciated. According to Dowson [71], there are some 22 muscles acting to move the femur, in our present model only abductor muscle was considered.

Femoral condyle which is the most distal cross section of the femur model were assumed to be fully fixed. In this study, single load bearing case representing single legged instance of a 750N human female.

The combined load is applied on the femoral head is by body weight and abductor muscles response. As femur is a thigh bone who shares the whole body weight equally by both the left and right femurs. In our study, single leg stance phase is considered so the actual body weight of 75 Kg (750 N) is applied on single side of femur according to hip mechanism.

$$\mathbf{M} = \mathbf{m} \times g \quad (6)$$

$$\mathbf{M} = 75 \times 10 = 750 \text{ N} \quad (7)$$

Where, m= mass of the subject, i.e., equals to 75 kg
& g= acceleration of gravity, i.e., equals to 10 m/s^2

The effect of this combined loading of body weight & the abductor muscle response required for equilibrium results in the loading of the femoral head to approximately 4 times body weight during the single leg stance phase of gait [70], [33].

For this analysis, most distal cross-section of the femur model i.e. area falling near femoral condyle were assumed to be fully fixed. Single load bearing case representing single legged instance of a 750N human female was taken for this study.

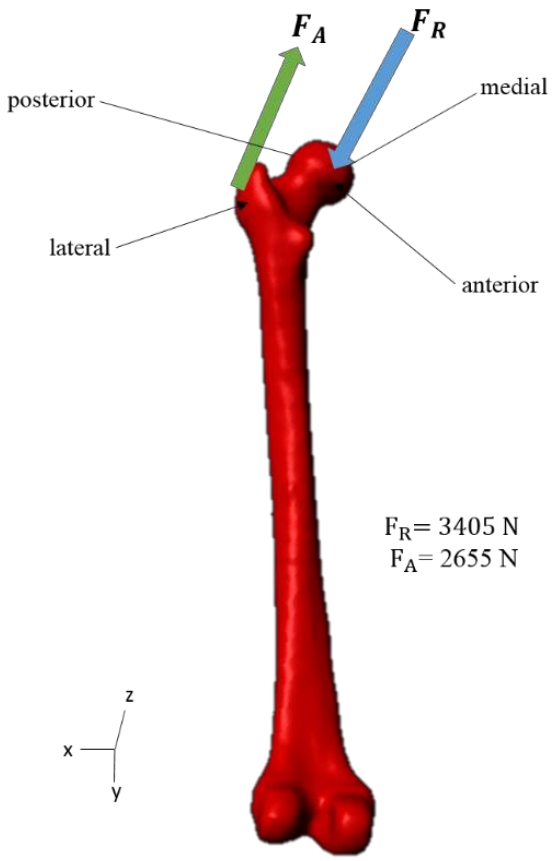

Figure 4.11. Schematic diagram of forces of muscles & body weight considered to be acting on the femur during single leg stance phase. F_R: represents the force on femoral head, F_A: represents the abductor muscles & controls the stability of the joint in the coronal plane.

Magnitude & direction of forces on femoral head were X: -915N, Y: -1,492N, Z:-

2,925N, and the resultant force on the femoral head was 4.54 body weight (BW).

$$F_R = 4.54 \times B_W = 4.54 \times M = 4.54 \times 750 = 3405\ N \quad (8)$$

Magnitude and direction of forces by abductor muscles were X: 832N, Y: -1,342N, Z: -

2,055N, and the resultant force was 3.54 body weight (BW).

$$F_A = 3.54 \times B_W = 3.54 \times M = 3.54 \times 750 = 2655\ N \quad (9)$$

5. RESULTS AND DISCUSSION

A 3D model of the intact femur was obtained from the CT image of the female subject and various measurements made using ScanIP tools. Measurements such as length, angle of inclination, volume, volume fraction and surface area are calculated using ScanIP, shown in Table 5.1.

Parameter	Subject **(F, 56 yrs.)**
Length of femur(mm)	390.95
Angle of inclination(degree)	122.01
Volume(mm^3)	238.136e3
Volume fraction (%)	2.59037
Surface area(mm^2)	60.5572e3

Table 5.1. Measured parameters of the model using ScanIP.

At the end of simulation, 3D solid model of intact femur in Creo 2.0 was analyzed using the F.E. package ANSYS 14.5 for the static loading. This study investigates mechanical parameters like equivalent von-Mises stress, maximum principal elastic strain, total deformation and maximal principal stress. On the value scale, the higher values are indicated by red color and the lower values are indicated by blue color. The values increase from blue to red. The results depend on the precision of FE model with respect to the real physiological conditions around the model.

Equivalent von Mises stress with a maximum value of 27588Pa was observed at the femoral shaft, as shown in Figure 5.1. and minimum value 42.455Pa was observed in between femoral head and neck of the femur , obtained from stress analysis of femur.

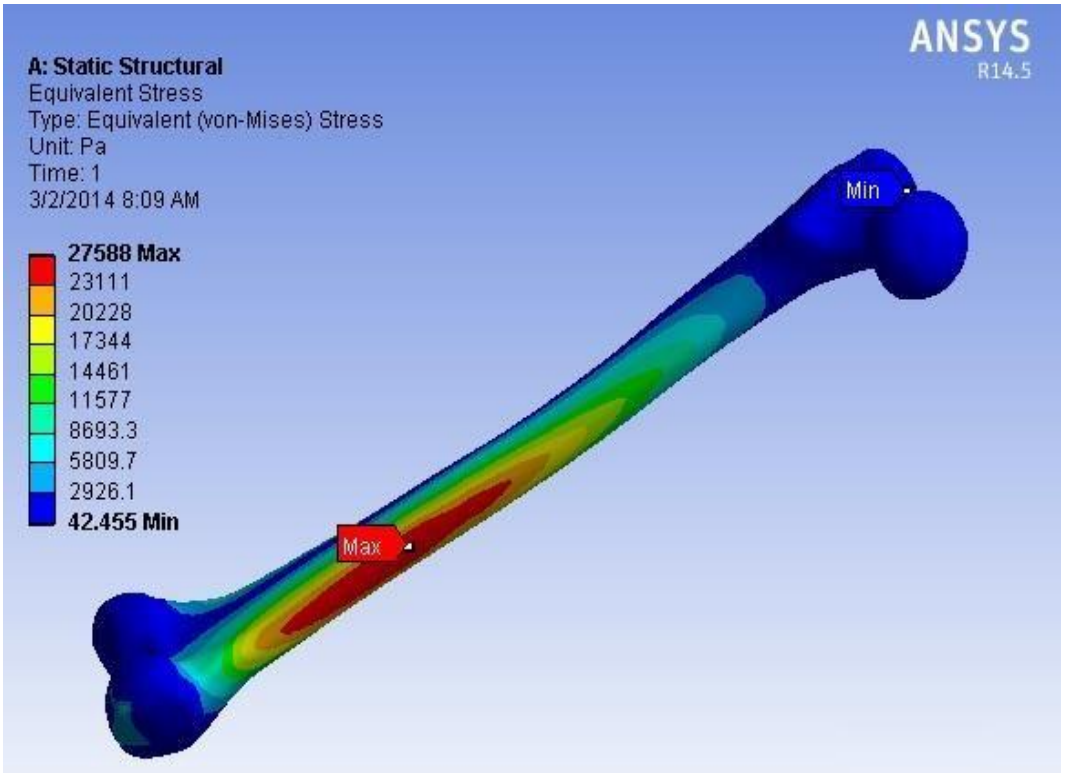

Figure 5.1. Equivalent von-Mises stress in femur.

Maximal principal elastic strain for the value of .0012968 almost negligible which occurred at distal side of femoral shaft, as shown in Figure 5.2.

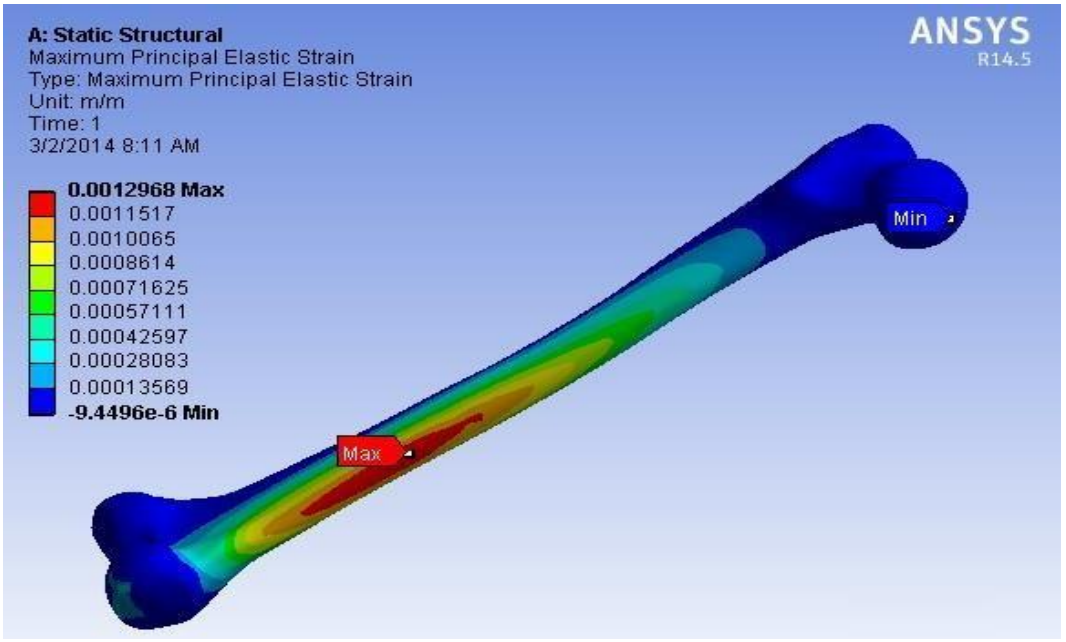

Figure 5.2. Maximum principal elastic strain in femur.

Maximum deformation in femur was .0048566m. Figure 5.3., occurred at femoral head which indicates a critical location in a femur for the specified subject while minimum deformation, 0m, was occurred at the condylar region of femur as it is the fixed end during the analysis. The figure shows that the deformation value decreases linearly with the cross section of femur from femoral head to the condylar region.

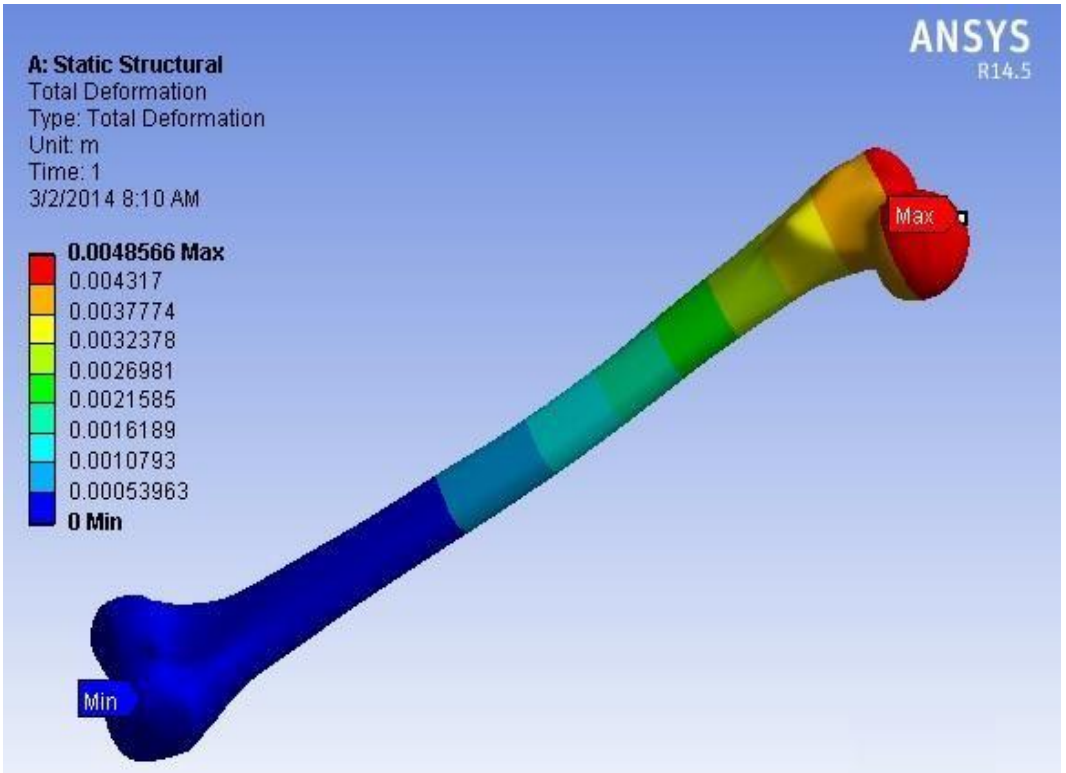

Figure 5.3. Maximum total deformation in femur.

Figure 5.4. showed that Maximum Principal Stress was observed at the shaft of the femur with a value of 1.2824e9 Pa and minimum value -3.105e7 Pa is observed at the neck of the femur.

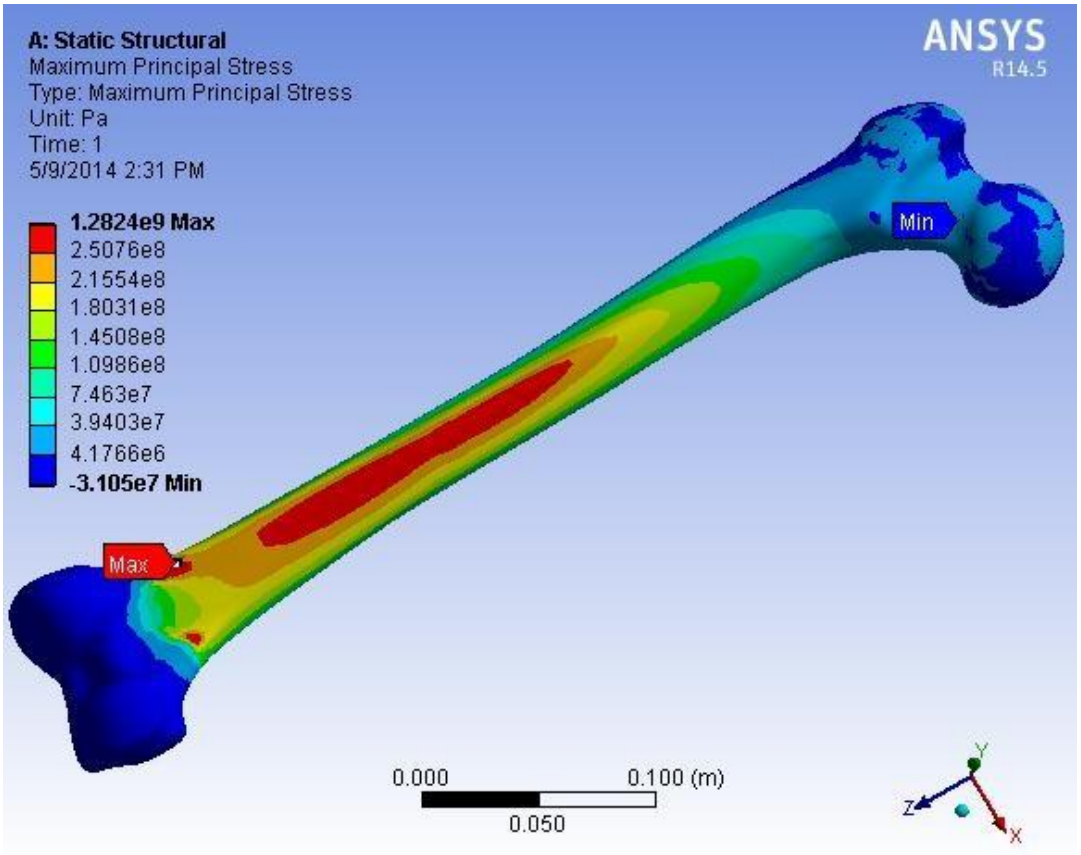

Figure 5.4. Maximum Principal Stress in Femur.

The comparison of these results was done with various literature reported. The behavior of our results was similar to behavior of results reported in literature. Slight variations associated with these mechanical behavior of femur was found due to high variation in material property and other physiological conditions.

Using this modeling approach, a next course of action, considering total hip replacement, implant designing, implant fitting and fracture treatment may be undertaken.

In orthopedic biomechanics, a number of approaches have been used to extract the geometry of interest from CT images such as MIMICS (Materialise Interactive Medical Image Control System), 3D Slicer, ScanIP and Amira. A drawback of these approaches is that their virtual memory usage is very high and as well as due to large size of DICOM file, when memory is not sufficient, the whole processing slows down. Therefore, high virtual memory computers are helpful to cut down this problem and also recommended to crop and resample the image so software will be able to process fast. The 3D FE model of femur bone generated from CT data has spark of interest because of its high importance in clinical practice. The problem is one of creating a valid and accurate model which satisfactorily represents the real structural behavior of the human bone. By selecting appropriate Window width-level (W, L) and greyscale values would help in getting better segmentation which will result in a better model. Manual segmentation needs expertise or practice to get satisfactory results.

6. CONCLUSION AND FUTURE WORK

CONCLUSION

In this research, various literatures related to the problem statement have been studied and generation of full solid model & static structural analysis of femur was done. This whole process includes generation of 3D model from quantitative CT scan images, NURBS meshing, assigning material properties, applying loading & boundary conditions and analyzing the model.

After going through various literatures and from this study, it was found that the extraction of geometry of interest from CT image by using segmentation technique is the most laborious step. And if better segmentation and smoothing is done, meshing process will be easy and a good solid model will be generated.

In this study, the internal zones of 3D solid model corresponding to cancellous bone, is further divided into two sub-zones of distal & proximal layer of femur, which is a better approximation of FE model with a real femur bone. However, this method has several issues that need improvement as this study is limited to the effect of one muscle and femur bone. Since the real anatomical structure of femur bone includes hard and soft tissue with bone marrow. Also, the physical conditions around the joint are much more complex as compared to this model, i.e., area around femoral head, neck and condylar region. Simulating all these issues, this work may be considered as a starting phase of computational analysis of biological structures by applying finite element method.

FUTURE SCOPE

In the study of joint biomechanics one of the primary issues of using finite element method is that it is very time consuming to segment surface geometry from medical image data, which potentially limits the amount of subjects that could be analyzed in a given study. Results of analysis and developed models are profitable for the orthopedic surgeons to understand the mechanical behavior of the femur bone, in hip replacement surgeries and implant designing & fixation. Method for developing a real femur model and the developed model itself can also be used as a data base for the forthcoming students who are interested to do further work in this area of biomechanics.

It would be more challenging to develop a more real type femur model, apart from cortical and cancellous bone, which also includes other hard and soft tissues. Developing a detailed 3D structure of femur is a problem that needs deeper consideration, given the issues observed. Also, the behavior of femur bone should be analyzed considering the physiological conditions around the bone joint.

REFERENCES

[1]http://www.iofbonehealth.org/factsstatistics

[2]http://articles.timesofindia.indiatimes.com/2010-06-07/india/28314801_1_hip-fractures-asian-audit-bad-bone-health 2010(July)

[3] http://www.uchospitals.edu/online-library/content=P08957 , Online Library, The University of Chicago Medicine.

[4] Wiiliam H. Harris and Clement B. Sledge, "Total Hip and Total Knee Replacement," The New England Journal of Medicine, 1990, v. 323, n. 11, pp. 725-731.

[5] http://www.surgeryinindia.in/hip-surgery-in-india.php

[6]http://ard.bmj.com/content/56/8/455.
full

[7] H. Malchau and P. Herberts, "Prognosis of total hip replacement," American Academy of Orthopedic Surgeons, New Orleans, USA, 1998.

[8] P. Cardiff, A. Karac, D. FitzPatrick, R. Flavin, and A. Ivankovic, "Development of a Hip Joint Model for Finite Volume Simulations," Journal of Biomechanical Engineering, 2014, v. 136, pp. 1-8.

[9] T. W. Pfeiler, D. S. Lalush, and E. G. Loboa, "Semiautomated finite element mesh generation methods for a long bone," Computer Methods Programs Biomed, 2007, v.85, pp. 196–202.

[10] A. A. Edidin, D. L. Taylor, and D. L. Bartel, "Automatic assignment of bone moduli from CT data: a 3-d finite element study," Proceedings of the 37th Annual Meeting of the Orthopedic Research Society, 1991, n. 16, pp. 491.

[11] B. Merz, P. Niedere, R. Muller, and P. Ruegsegger, "Automated finite element analysis of excised human femora based on precision-QCT," Journal of Biomechanical Engineering, 1996, v. 118, n. 3, pp. 387–390.

[12] M. Lengsfeld, J. Kaminsky, B. Merz, and R.P. Franke, "Sensitivity of Femoral Strain Pattern Analyses to Resultant and Muscle Forces at the Hip Joint," Journal of Medical Engineering Physics, 1996, v. 18, n. 1, pp. 70-78.

[13] A.E. Anderson, "Computational Modeling of Hip Joint Mechanics," D.Phil. Thesis,The University of Utah, US, 2007.

[14] J. Currey, The Mechanical Adaption of Bones, Princeton University Press, 1984.

[15] http://www.studyblue.com/notes/note/n/parts-of-a-long-bone/deck/5543113 Jackie S.

[16] D.R. Gore, M.P. Murray, G.M. Gardner, and S.B. Sepic, "Roentgenographic Measurements after Muller Total Hip Replacement. Correlations among Roentgenographic Measurements and Hip Strength and Mobility," Journal of Bone Joint Surgery Am, 1977, v. 59, pp. 948-53.

[17] N. Özkaya, M. Nordin, D. Goldsheyder, and D. Leger, "Fundamentals of Biomechanics: Equilibrium, Motion, and Deformation," (3rd Edition), Springer, New York, USA, 2012.

[18] Eldra P. Solomon, Richard R. Schmidt, and Peter J. Adragna, Human anatomy &physiology (2nd edition), Sunders College Publishing, Philadelphia, US, 1990.

[19] H. Gray, Gray's Anatomy of the Human Body, (20th edition), Lea and Febiger, Philadelphia, US, 1918.

[20] G.J. Tortora, B.H. Derrickson, Principles of Anatomy and Physiology, (12thedition), Wiley, New York, US, 2008.

[21] George L. Lucas, Francis W. Cooke, Elizabeth Friis and D.Y. Chinn, A Primer of Biomechanics, Springer, New York, USA, 1999.

[22] N. Hamilton, W. Weimar, K. Luttgens, Kinesiology: Scientific Basis of Human Motion, McGraw Hill Higher Education, 2007, pp. 147-162.
[23] "Functional Anatomy of the Hip Joint," Ch7 pdf file, pp. 237-
250.

[24] S. Mann, "Molecular tectonics in bio mineralization and biomimetic materials chemistry," Nature, 1993, n. 365, 499–505.

[25] J.D. Currey, "Hierarchies in biomineral structures," Science, PubMed, 2005, v. 309, pp. 253.

[26] J.C. Elliott, "Structure and chemistry of the apatites and other calcium orthophosphates," Elsevier, Amsterdam, Netherlands, 1994.

[27] J.C. Elliott, "Calcium phosphate biominerals," In: Kohn MJ, Rakovan J, Hughes JM, (eds.) Phosphates: geochemical, geobiological and materials importance, reviews in mineralogy and geochemistry, Mineral Society of America, Washington DC, US, 2002, v. 48, pp. 427–453.

[28] D.T. Reilly, and A.H. Burstein, "The elastic and ultimate properties of compact bone tissue," Journal of Biomechanics, v. 8, pp. 393-405, 1975.

[29] D.R. Carter, and W.C. Hayes, “Fatigue life of compact bone l: Effects of stress
amplitude, temperature and density,” Journal of biomechanics, 1997a, v. 9, pp. 27-34.

[30] J.C. Lotz, E.J. Cheal, and W.D. Hayes, “Fracture prediction for the proximal femur using finite element models. Part I: Linear analysis. Part II: Nonlinear analysis,” Journal of Biomechanical Engineering, 1991, v. 113, pp. 353-365.

[31] R.V. Mises, “Mechanik der festen Körper im plastisch deformablen Zustand,” Göttin. Nachr, Math.-Phys., 1913, v.1, pp. 582–592.

[32]http://www.learnengineering.org/2012/12/what-is-von-mises-stress.html

[33] F. Pauwels, Biomechanics of the Locomotor Apparatus, Springer-Verlag, New York, 1980, pp. 1-228.

[34]http://aboutjoints.com/physicianinfo/topics/anatomyhip/biomechanicship.html

[35] M.J. Fagan, and A.J.C. Lee, “Material selection in the design of the femoral component of cemented total hip replacements,” Clinical Materials, 1986, v. 1, pp. 151-167.

[36] E.Y. Chao, and K.N. An, “Biomechanical analysis of external fixation devices for the treatment of open bone fractures in finite element,” in Biomechanics, R.H. Gallagher, B.R. Simon, P.C. Johnson, and J.F. Gross (eds.), John Wiley & Sons, New York, 1982.

[37] N.S. Gokhale, S.S. Deshpande, S.V. Bedekar, and A.N. Thite, Practical Finite Element Analysis, Finite to Infinite, (1st Edition), Pune, Maharashtra, India, 2008.

[38]http://www.sv.vt.edu/classes/MSE2094_NoteBook/97ClassProj/num/widas/history.html

[39] http://www.brighthubengineering.com/cad-autocad-reviews-tips/66732-what-are- the-steps-required-to-perform-a-finite-element-analysis/

[40] H.M. Frost, Bone modeling & skeletal modeling errors. Orthopedics Lectures, Springfield, Illinois, 1973.

[41] M.E. Taylor, K.E. Tanner, M.A.R. Freeman, and A.L. Yettram, “Stress & Strain distribution within the intact femur: compression or bending?,” Medical Eng. Physics,1996, v. 18, n. 2, pp. 122-131.

[42] A. Dabrowska-Tkaczyk, M. Pawlikowski, "Influence of remodeling, stimulating factor selection on bone density distribution in pelvic bone model," Acta of Bioengineering and Biomechanics, 2006, v. 8, n. 2, pp. 119-126.

[43] C. Radu, and I.C. Rosca, "Modeling of the Hip Joint," Annals of the Ordea university, Fascicle of Management and Technological Engineering, 2007, v. VI (XVI), pp. 745-750.

[44] M.O. Ghiba, and L. Rusu, "Geometrical design of custom-made femoral stem prostheses," Annals of the Ordea university, Fascicle of Management and Technological Engineering, 2008, v. VII (XVII), pp. 835-840.

[45] Z. Jun-hai, M. Shu-fang, and W. Xue-ying, "Finite Element Analysis of Femur Stress under Bending Moment and Compression Load," IEEE, 2009, pp. 1-4.

[46] M.D. Trajanovic, N.M. Vitkovic, M.S. Stojkovic, M.T. Manic, and S.D. Arsic, "The Morphological Approach to Geometrical Modeling of the Distal Femur," 2nd South-East European Conference on Computational Mechanics, Rhodes, Greece, 2009, pp. 1-8.

[47] M.O. Ghiba, R. Prejbeanu, and D. Vermesan, "Finite Element Model Analysis of Coxofemoral Joint Using Composite Materials," (Short communication), Materiale Plastice, 2010, v. 47, n. 1, pp. 115-116.

[48] R. Nareliya, and V. Kumar, "Biomechanical Analysis of Human Femur Bone,"International Journal of Engineering Science and Technology, 2011, v. 3, n. 4, pp. 160-166.

[49] A.R. Shinge, S.S. Anasane, E.N. Aitavade, S.S. Mahadik, and P. Mulik, "Finite Element Analysis of Modified Hip Prosthesis," 2011, v. 2, n. 2, pp. 278-285.

[50] S. Vulovic, N. Korunovic, M. Trajanovic, N. Grujovic, and N. Vitkovic, "Finite element analysis of CT based femur model using finite element program PAK," Journal of the Serbian Society for Computational Mechanics, 2011, v. 5, n. 2, pp. 160-166.

[51] S. Lahari M, Vijay, and Anburajan M, "Finite Element Analysis of Femur in the Evaluation of Osteoporosis," IEEE, 2011, pp. 415-419.

[52] A. Francis, and V. Kumar, "Computational Modeling of Human Femur using CT Data for Finite Element Analysis," International Journal of Engineering Research & Technology, 2012, v. 1, n. 6, pp. 1-7.

[53] K.V. Datar, Y.P. Reddy, and R. Sarangapani, "Fatigue life analysis of partial hip endoprosthesis for an activity of brisk walking," International Journal of Engineering Research and Applications, 2012, v. 2, n. 6, pp.

[54] L. de F. Spinelli, C.A. de S. Macedo, C.R. Galia, R. Rosito, F. Schnaid, L.L. Corso, and I. Iturrioz, "Femoral stem-bone interface analysis of logical uncemented stem," Engenharia Biomedica, Brazilian Journal of Biomedical Engineering, 2012, v. 28, n. 3, pp. 238-247.

[55] Y. Shireesha, S. V. Ramana, and P.G. Rao, "Modeling and static analysis of femur bone by using different implant materials," IOSR Journal of Mechanical and Civil Engineering, 2013, v. 7, n. 4, pp. 82-91.

[56] R. Ghosh, B. Pala, D. Ghosh, and S. Gupta, "Finite element analysis of a hemi-pelvis: the effect of inclusion of cartilage layer on acetabular stresses and strain," Computer Methods in Biomechanics and Biomedical Engineering, Taylor & Francis Group, London, UK, 2013, pp. 1-14.

[57] N.K. Singh, R. Braru, and S.K. Rai, "Development and Validation of Robust 3D Solid Model of Femur Using CT Data," IRF International Conference, Goa, India, 2014, pp. 51-55.

[58] L. Peng, J. Bai, X. Zeng, and Y. Zhou, "Comparison of isotropic and orthotropic material property assignments on femoral finite element models under two loading conditions," Medical Engineering Physics, 2007, n. 28, pp. 227–233.

[59] http://www.simpleware.com/software/scanip/, ScanIP 6.0 (Tutorial and Reference Guide), Simpleware, 2013.

[60] Ed Sutton, "Histograms and the Zone System," Illustrated Photography.

[61] S. Johnson, "Stephen Johnson on Digital Photography," O'Reilly Media Inc, 2006. ISBN 0-596-52370-X.

[62] K.E. Rudman, R.M. Aspden, and J.R. Meakin, "Compression or tension? The stress distribution in the proximal femur," BioMedical Engineering OnLine, BioMed Central, 2006, pp. 1-7.

[63] B. van Rietbergen, R. Huiskes, F. Eckstein, and P. Ruegsegger, "Trabecular bone tissue strains in the healthy and osteoporotic human femur," Journal of Bone and Mineral Research, 2003, v. 18, pp. 1781-1788.

[64] C. Bitsakos, J. Kerner, F. Fisher, and A.A. Amis, "The effect of muscle loading on the simulation of bone remodeling in the proximal femur," Journal of Biomechanics,
2005, v. 38, pp. 133-
139.

[65] E. Verhulp, B. van Rietbergen, and R. Huiskes, "Comparison of micro-level and continuum level voxel models of the proximal femur," Journal of Biomechanics, 2006, v. 39, pp. 2951-2957.

[66] Z. Jiang-jun, Z. Min, Y. Ya-bo, L. Wei, L. Ren-fa, Z. Zhi-yu, C. Rong-jian, Y. Wei-tao, and D. Cheng fei, “Finite element analysis of a bone healing model: 1-year follow-up after internal fixation surgery for femoral fracture,” Pak Journal Medical Science, 2014, v. 30, n. 2, pp. 1-5.

[67] H.B. Jiang, and S.R. Ge, “Human femur finite element analysis based on CT scan data,” Engineering Mechanics, paper 24, p. 156-159.

[68] J.P. Paul, "Loading on normal hip and knee joints and on replacements," in Advances in artificial hip and knee joint technology, D. Holmann, and M. Schaldach (eds.), Eng. In Med 2, 1976.

[69] J.P. Paul, "Approaches to design. Force actions transmitted by joints in the human body," Proceedings R. Soc. Lond. B., 1976b, paper 192, pp. 163-172.

[70] G. Bergmann, G. Deuretzbacher, M. Heller, F. Graichen, A. Rohlmann, J. Strauss and G.N. Duda, “Hip Contact Forces and Gait Pattern from Routine Activities,” Journal of Biomechanics, Elsevier, 2001, v. 34, pp. 859-871.

[71] D. Dowson, "Bio-mechanics of the lower limb," In An introduction to biomechanics of joints and joint replacements, D. Dowson, and V. Wright (eds.), MEP, London, 1981, pp. 68-73.

APPENDICES

APPENDIX A

Physical and imaging property of all three masks from ScanIP were given in Table.

Surface Mask (mm^2) (Original)	Mean Voxel Count (Original)	Std. Deviation Volume (mm^3) Grayscale	Area	Pixel Values	Grayscale of	
Red Mask (Cortical)	492,089	252E3	92.5E3	13.58-787.35	127	87.2
Turquoise Mask (Cancellous at distal end)	141,502	72.4E3	23.1E3	-26.44-500	52.6	33.9
Green Mask (Cancellous at proximal end)	76,805	39.3E3	15.8E3	1-270	68.7	37.9
Sum(All 3 mask)	710,396	364E3	131E3	-26.44-787.35	-	-